located on Chromosome 6) is higher than usual due to the need for appropriate considerations of previously reported variants on the same chromosome. It is reassuring to note that both *C6orf223* and *SLC44A1* showed the strongest two signals of association with AMD outside of *CFH*, *ARMS2-HTRA1* and *CETP*. Our exhaustive analyses using logistic regression adjusting for allele dosages at previously described SNP markers suggest that both *C6orf223* and *SLC44A1* are unrelated to those previously reported, and thus they likely represent Asian-specific genetic associations for AMD.

Neither *FGD6* nor the genes within its vicinity (Fig. 2c) have ever been previously implicated in any ocular disorders. *FGD6* encodes for FYVE, RhoGEF and PH domain-containing protein 6, with its functions yet to be characterized. The Q257R mutation is less than half as common in Europeans (MAF = 0.10) compared with East Asians (MAF = 0.20–0.30), again possibly explaining the ability of our study to pick up this genetic effect.

The identified genes were expressed in human retinal pigment epithelium (Supplementary Table 11). Of the three non-synonymous substitutions, the *CETP* D442G variant was predicted by both PolyPhen[36] and SIFT[37] to likely be causing damage to the protein structure/function, the *FGD6* Q257R variant was predicted only by PolyPhen to be probably damaging but by SIFT to be tolerated and the *SLC44A4* D47V variant was predicted by both tools to be benign or tolerated. Although the use of both prediction algorithms has been reported to be moderately sensitive, they suffer from lack of specificity[38], and thus more evidence should be sought with regards to the *FDG6* and *SLC44A4* non-synonymous variants.

Using HaploReg[39], RegulomeDB[40] and Encyclopaedia of DNA Elements (ENCODE)[41] data, we identified variants within each of the four LD blocks in the 1000 Genomes Project ($r^2 > 0.8$ and <250 kb from the top SNP) to apply functional annotations relevant to the regulation of transcription (Supplementary Table 12). In addition to their functions on amino-acid substitutions, all of the four identified variants lie within a DNase I hypersensitivity site or in a region where modification of histones is suggestive of promoter, enhancer and other regulatory activity, and/or have an influence on binding of transcription factors or effects on a specific regulatory motif. *C6orf223* A231A (rs2295334) and *FGD6* Q257R could tag genetic variants that lie in potential transcription-factor binding sites (Supplementary Table 13). Examination of a recently available large-scale eQTL mapping database[42] indicates that out of the four novel genome-wide significant SNPs, markers *SLC44A4* D47V and *FDG6* Q257R could serve as cis-eQTLs. The minor allele at *SLC44A4* D47V (rs12661281) is associated with significantly altered expression of HSPA1B and CSKN2B, which are located within a 210,000 bp region flanking *SLC44A4* D47V. The minor allele at *FDG6* Q257R (rs10507047) is associated with significantly increased expression of the neighbouring *VEZT* gene (Supplementary Table 14). Given that these findings are based on expression in whole blood in European samples, further work will be needed to elucidate their role in retinal tissue and in Asian samples. Nonetheless, these could suggest possible alternate mechanisms whereby both non-synonymous substitutions potentially affect AMD risk apart from directly affecting the protein structure of their parent genes.

Our study examined mainly the exudative subtype of AMD, and therefore cannot be completely compared with other studies looking at advanced AMD including the choroidal neovascularization and geographic atrophy subtypes. We also note substantial differences in inter-ethnic MAF for most of the previously reported loci associated with AMD in European-ancestry populations (Supplementary Table 1). This could represent genuine differences in genetic architecture in AMD between Asians and Europeans, or that the low allele frequency in either ethnicity could result in insufficient power to replicate genome-wide significant hits initially observed in either Asians or Europeans. Overall, out of 21 previously reported SNPs showing strong evidence of association in Europeans, we were able to replicate 9 of them in our study of East Asians at $P<0.05$. Taken together with the three novel loci and one novel variant in *CETP* in East Asians discovered in this study, we postulate that the genetic mechanisms of AMD in Asians could, in part, be somewhat distinct from that in Europeans.

In summary, our genome-wide and exome-wide study of AMD provides new insights into the genetic mechanisms of AMD in East Asians. Our study highlights the value of searching for low-frequency, ethnic-specific genetic variants on the coding frame of AMD that may inform pathogenesis. Although some of the genetic loci conferring disease susceptibility in East Asians are shared with Europeans (for example, common variation mapping to *CFH*, *HTRA1* and *CETP*), we identified significant important differences in the fine-scale genetic architecture of AMD, which appear specific to East Asians. Such differences could underpin at least some of the inter-ethnic differences in clinical presentation and response to specific therapies, including the poorer response to anti-VEGF therapy in Asians.

Methods

Study design and phenotyping. We performed a GWAS and EWAS on neovascular AMD in East Asians. In the discovery stage, we included and genotyped 2,119 cases and 5,691 controls from three case–control studies from Singapore, Hong Kong and Japan. For replication, five independent case–control studies were conducted in Korea, Japan, and Guangdong, Sichuan and Beijing in China, totalling 4,226 cases and 10,289 controls. All the studies were performed with the approval of their local Medical Ethics Committee, and written informed consent was obtained from all the participants in accordance with the Declaration of Helsinki.

A detailed description of subject recruitment and phenotyping in each sample collection is provided in Supplementary Methods, and summarized in Table 1. In brief, the diagnosis of exudative AMD was made at each site by retinal specialists, according to standard clinical definitions on the basis of detailed ophthalmic examinations, including dilated fundus photography, fluorescein angiography, indocyanine green angiography and optical coherence tomography (Table 1). Grading of fluorescein angiograms for the presence of choroidal neovascularization were performed using a modification from the Macular Photocoagulation Study[43]. Indocyanine green angiography was performed to diagnose definitive polypoidal choroidal vasculopathy, a variant of AMD, using the Japanese Study Group guidelines[44]. Cases with other macular diseases such as central serous chorioretinopathy, high myopia and angioid streaks were excluded. Of the 2,119 exudative AMD cases included in the discovery phase, 1,083 (51%) were classified as 'typical neovascular AMD', 1,015 (48%) were polypoidal choroidal vasculopathy and 21 (1%) had one eye with typical neovascular AMD and the other eye with polypoidal choroidal vasculopathy. At each site, controls subjects without any clinical signs of AMD were either recruited from eye clinics or enrolled from population-based studies (Supplementary Methods).

Genotyping and imputation. For the discovery stage, GWAS genotyping was performed using the Illumina Human OmniExpress or Human Hap610-Quad beadchips, and EWAS was done using HumanExome beadchips (Table 1). For replication, genotyping was performed using the MassArray platform (Sequenom), as well as using Taqman allelic discrimination probes (Applied Biosystems).

Stringent quality control filters were used to remove poorly performing samples and SNP markers in both the discovery and replication (de-novo genotyping) phases. For the GWAS, SNPs with a call rate of $<95\%$, MAF of $<1\%$, or showing deviation from Hardy–Weinberg Equilibrium ($P<10^{-6}$) were removed from further statistical analysis. For the EWAS, SNPs with a call rate of $<99\%$, MAF of $<0.1\%$ or showing deviation from equilibrium ($P<10^{-6}$) were removed. The 99% threshold was used as many SNP markers on the exome array had MAF $<5\%$, and as such, differential genotyping success rates between cases and controls as low as 2% could result in false-positive findings. SNPs which were not monomorphic (whereby at least one heterozygous carrier individual was present) were included for downstream analysis.

Routine quality control criteria on a per-sample basis were carried out, and poorly performing samples were removed from further analysis. The remaining samples were then subjected to biological relationship verification by using the principle of variability in allele sharing according to the degree of relationship. Identity-by-state information was derived using the PLINK software[45]. For those pairs of first-degree relatives so identified (for example, parent–offspring, full-

siblings, as well as monozygous twins), we removed the sample with the lower call rate before performing PC analysis.

The imputation was carried out using IMPUTE2 version 2.2.2 with ASN population haplotypes from 1000 Genomes as reference, as described elsewhere[46–48]. Imputed genotypes were called with an impute probability threshold of 0.9 with all other genotypes classified as missing. Additional quality control filters were applied to remove SNPs with >1% missingness should the SNP have a MAF <5% in either cases or controls. For common SNPS with MAF >5%, the filtering criteria were set at >5% missingness.

Statistical analysis. For the discovery stage, all exudative AMD cases and controls appear well matched when visualized spatially on PC analysis for each sample collection on a per-country basis for Hong Kong, Japan and Singapore and according to self-reported ethnicity (ethnic Chinese for Hong Kong and Singapore, and ethnic Japanese for Japan; Supplementary Fig. 6), using previously reported criteria[49], indicating that population stratification is unlikely to confound the association results.

For both the discovery and replication stages, analysis of association with exudative AMD was carried out using 1-degree of freedom score-based tests using logistic regression. The tests model for a trend-per-copy effect of the minor allele on disease risk. For the discovery stage, we incorporated the top five PCs of genetic stratification into the logistic regression model to minimize the effect of residual population stratification[50]. We could not adjust for population stratification for the replication stage due to limited number of SNPs tested. Meta-analysis was conducted using inverse variance weights for each sample collection, which calculates an overall Z-statistic, corresponding *P* value and accompanying per-allele OR for each SNP analysed. Gene-based tests on mutational load was performed using the SKAT-O test[16]. The association between *CETP* D442G and serum HDL-c level was assessed using linear regression assuming an additive model of inheritance as previously described[23] (due to serum HDL-c being distributed normally), with adjustment for age, gender and body mass index.

Regional association and PC plots were analysed and plotted using the R statistical software package.

Power calculations. For the discovery stage (2,119 AMD cases and 5,691 controls), power calculations[51] indicated that there is 80% power of detecting loci at $P<1\times10^{-4}$ (the threshold of association for bringing forward SNPs to the replication stage) at MAF as low as 10% with per-allele OR of 1.30. For rarer variants of higher penetrance, the discovery stage has 80% power of detecting loci at $P<1\times10^{-4}$ at MAF as low as 2% if the per-allele OR is at least 1.70. The entire sample (6,345 AMD cases and 15,980 controls) has 80% power to detect loci at $P<5.0\times10^{-8}$ at MAF as low as 2% if the per-allele OR is at least 1.55 or at MAF as low as 9% with per-allele OR of 1.25, in line with the effect sizes being reported in this study. Supplementary Table 15A shows the power calculations to detect SNPs at the threshold of $P<1\times10^{-4}$ in the discovery stage for bringing forward to the replication stage. Supplementary Table 15B shows the formal power calculations in the context of the combined discovery and replication stages.

References

1. Lim, L. S., Mitchell, P., Seddon, J. M., Holz, F. G. & Wong, T. Y. Age-related macular degeneration. *Lancet* **379,** 1728–1738 (2012).
2. Wong, W. L. *et al.* Global prevalence and burden of age-related macular degeneration: a meta-analysis and disease burden projection for 2020 and 2040. *Lancet Glob. Health* **2,** e106–e116 (2014).
3. Spencer, K. L. *et al.* Protective effect of complement factor B and complement component 2 variants in age-related macular degeneration. *Hum. Mol. Genet.* **16,** 1986–1992 (2007).
4. Chen, W. *et al.* Genetic variants near TIMP3 and high-density lipoprotein-associated loci influence susceptibility to age-related macular degeneration. *Proc. Natl Acad. Sci. USA* **107,** 7401–7406 (2010).
5. Yu, Y. *et al.* Common variants near FRK/COL10A1 and VEGFA are associated with advanced age-related macular degeneration. *Hum. Mol. Genet.* **20,** 3699–3709 (2011).
6. Fritsche, L. G. *et al.* Seven new loci associated with age-related macular degeneration. *Nat. Genet.* **45,** 433–439 439e431–432 (2013).
7. Raychaudhuri, S. *et al.* A rare penetrant mutation in CFH confers high risk of age-related macular degeneration. *Nat. Genet.* **43,** 1232–1236 (2011).
8. Seddon, J. M. *et al.* Rare variants in CFI, C3 and C9 are associated with high risk of advanced age-related macular degeneration. *Nat. Genet.* **45,** 1366–1370 (2013).
9. Helgason, H. *et al.* A rare nonsynonymous sequence variant in C3 is associated with high risk of age-related macular degeneration. *Nat. Genet.* **45,** 1371–1374 (2013).
10. Zhan, X. *et al.* Identification of a rare coding variant in complement 3 associated with age-related macular degeneration. *Nat. Genet.* **45,** 1375–1379 (2013).
11. Arakawa, S. *et al.* Genome-wide association study identifies two susceptibility loci for exudative age-related macular degeneration in the Japanese population. *Nat. Genet.* **43,** 1001–1004 (2011).
12. Laude, A. *et al.* Polypoidal choroidal vasculopathy and neovascular age-related macular degeneration: same or different disease? *Prog. Retin. Eye Res.* **29,** 19–29 (2010).
13. Cheung, C. M. & Wong, T. Y. Ranibizumab and bevacizumab for AMD *New Engl. J. Med.* **365,** 2237 author reply 2237 (2011).
14. van de Ven, J. P. *et al.* A functional variant in the CFI gene confers a high risk of age-related macular degeneration. *Nat. Genet.* **45,** 813–817 (2013).
15. Huyghe, J. R. *et al.* Exome array analysis identifies new loci and low-frequency variants influencing insulin processing and secretion. *Nat. Genet.* **45,** 197–201 (2013).
16. Lee, S., Wu, M. C. & Lin, X. Optimal tests for rare variant effects in sequencing association studies. *Biostatistics* **13,** 762–775 (2012).
17. Inazu, A. *et al.* Genetic cholesteryl ester transfer protein deficiency caused by two prevalent mutations as a major determinant of increased levels of high density lipoprotein cholesterol. *J Clin. Invest.* **94,** 1872–1882 (1994).
18. Barter, P. J. *et al.* Cholesteryl ester transfer protein: a novel target for raising HDL and inhibiting atherosclerosis. *Arterioscler. Thromb. Vasc. Biol.* **23,** 160–167 (2003).
19. Lavanya, R. *et al.* Methodology of the Singapore Indian Chinese Cohort (SICC) eye study: quantifying ethnic variations in the epidemiology of eye diseases in Asians. *Ophthalmic Epidemiol.* **16,** 325–336 (2009).
20. Sabanayagam, C. *et al.* Retinal arteriolar narrowing increases the likelihood of chronic kidney disease in hypertension. *J. Hypertens.* **27,** 2209–2217 (2009).
21. Cheung, C. M. *et al.* Prevalence of and risk factors for age-related macular degeneration in a multiethnic Asian cohort. *Arch. Ophthalmol.* **130,** 480–486 (2012).
22. Nakata, I. *et al.* Prevalence and characteristics of age-related macular degeneration in the Japanese population: the nagahama study. *Am. J. Ophthalmol.* **156,** 1002–1009 e1002 (2013).
23. Kathiresan, S. *et al.* Six new loci associated with blood low-density lipoprotein cholesterol, high-density lipoprotein cholesterol or triglycerides in humans. *Nat. Genet.* **40,** 189–197 (2008).
24. Kathiresan, S. *et al.* Common variants at 30 loci contribute to polygenic dyslipidemia. *Nat. Genet.* **41,** 56–65 (2009).
25. Hankin, J. H. *et al.* Singapore Chinese Health Study: development, validation, and calibration of the quantitative food frequency questionnaire. *Nutr. Cancer* **39,** 187–195 (2001).
26. Takeuchi, F. *et al.* Association of genetic variants influencing lipid levels with coronary artery disease in Japanese individuals. *PLoS ONE* **7,** e46385 (2012).
27. Takahashi, K. *et al.* A missense mutation in the cholesteryl ester transfer protein gene with possible dominant effects on plasma high density lipoproteins. *J. Clin. Invest.* **92,** 2060–2064 (1993).
28. Freeman, D. J. *et al.* A polymorphism of the cholesteryl ester transfer protein gene predicts cardiovascular events in non-smokers in the West of Scotland Coronary Prevention Study. *Eur. Heart J.* **24,** 1833–1842 (2003).
29. Howard, B. V. *et al.* LDL cholesterol as a strong predictor of coronary heart disease in diabetic individuals with insulin resistance and low LDL: The Strong Heart Study. *Arterioscler. Thromb. Vasc. Biol.* **20,** 830–835 (2000).
30. Grundy, S. M. Low-density lipoprotein, non-high-density lipoprotein, and apolipoprotein B as targets of lipid-lowering therapy. *Circulation* **106,** 2526–2529 (2002).
31. Hara, R. *et al.* Photodynamic therapy alone versus combined with intravitreal bevacizumab for neovascular age-related macular degeneration without polypoidal choroidal vasculopathy in Japanese patients. *Graefes Arch. Clin. Exp. Ophthalmol.* **248,** 931–936 (2010).
32. Kumar, V. *et al.* Genome-wide association study identifies a susceptibility locus for HCV-induced hepatocellular carcinoma. *Nat. Genet.* **43,** 455–458 (2011).
33. Su, Z. *et al.* Common variants at the MHC locus and at chromosome 16q24.1 predispose to Barrett's esophagus. *Nat. Genet.* **44,** 1131–1136 (2012).
34. O'Regan, S. *et al.* An electric lobe suppressor for a yeast choline transport mutation belongs to a new family of transporter-like proteins. *Proc. Natl Acad. Sci. USA* **97,** 1835–1840 (2000).
35. Uhl, J. *et al.* Identification of a CTL4/Neu1 fusion transcript in a sialidosis patient. *FEBS Lett.* **521,** 19–23 (2002).
36. Adzhubei, I. A. *et al.* A method and server for predicting damaging missense mutations. *Nat. Methods* **7,** 248–249 (2010).
37. Ng, P. C. & Henikoff, S. SIFT: predicting amino acid changes that affect protein function. *Nucleic Acids Res.* **31,** 3812–3814 (2003).
38. Flanagan, S. E., Patch, A. M. & Ellard, S. Using SIFT and PolyPhen to predict loss-of-function and gain-of-function mutations. *Genet. Test. Mol. Biomarkers* **14,** 533–537 (2010).
39. Ward, L. D. & Kellis, M. HaploReg: a resource for exploring chromatin states, conservation, and regulatory motif alterations within sets of genetically linked variants. *Nucleic Acids Res.* **40,** D930–D934 (2012).

40. Boyle, A. P. *et al.* Annotation of functional variation in personal genomes using RegulomeDB. *Genome Res.* **22,** 1790–1797 (2012).
41. Consortium, E. P. *et al.* An integrated encyclopedia of DNA elements in the human genome. *Nature* **489,** 57–74 (2012).
42. Westra, H. J. *et al.* Systematic identification of trans eQTLs as putative drivers of known disease associations. *Nat. Genet.* **45,** 1238–1243 (2013).
43. Laser photocoagulation of subfoveal neovascular lesions in age-related macular degeneration. Results of a randomized clinical trial. Macular Photocoagulation Study Group. *Arch. Ophthalmol.* **109,** 1220–1231 (1991).
44. Japanese Study Group of Polypoidal Choroidal, V. [Criteria for diagnosis of polypoidal choroidal vasculopathy]. *Nihon Ganka Gakkai Zasshi* **109,** 417–427 (2005).
45. Purcell, S. *et al.* PLINK: a tool set for whole-genome association and population-based linkage analyses. *Am. J. Hum. Genet.* **81,** 559–575 (2007).
46. Marchini, J., Howie, B., Myers, S., McVean, G. & Donnelly, P. A new multipoint method for genome-wide association studies by imputation of genotypes. *Nat. Genet.* **39,** 906–913 (2007).
47. Howie, B. N., Donnelly, P. & Marchini, J. A flexible and accurate genotype imputation method for the next generation of genome-wide association studies. *PLoS Genet.* **5,** e1000529 (2009).
48. Howie, B., Fuchsberger, C., Stephens, M., Marchini, J. & Abecasis, G. R. Fast and accurate genotype imputation in genome-wide association studies through pre-phasing. *Nat. Genet.* **44,** 955–959 (2012).
49. Vithana, E. N. *et al.* Genome-wide association analyses identify three new susceptibility loci for primary angle closure glaucoma. *Nat. Genet.* **44,** 1142–1146 (2012).
50. Khor, C. C. *et al.* Genome-wide association study identifies FCGR2A as a susceptibility locus for Kawasaki disease. *Nat. Genet.* **43,** 1241–1246 (2011).
51. Purcell, S., Cherny, S. S. & Sham, P. C. Genetic Power Calculator: design of linkage and association genetic mapping studies of complex traits. *Bioinformatics* **19,** 149–150 (2003).

Acknowledgements

We thank the staff and participants of all studies for their important contributions. This research was supported by the National Medical Research Council (NMRC grants 0796/2003, IRG07nov013, IRG09nov014, NMRC 1176/2008, NIG/1003/2009, STaR/0003/2008, CG/SERI/2010 and CSA/033/2012), and Biomedical Research Council (BMRC 08/1/35/19/550, 09/1/35/19/616 and 10/1/35/19/671) in Singapore; BrightFocus Foundation (M2011068), USA; the Seoul National University Bundang Hospital Research Grant Fund (grant no. 03-2009-008), and National Research Foundation of Korea (NRF-2009-0072603, NRF-2012R1A1A2008943, NRF-2014R1A2A1A09005824) grants funded by the Ministry of Education, Science and Technology, Korea; and grants-in-aid for scientific research (No. 24249082) from the Japan Society for the Promotion of Science, Tokyo, Japan; the National Natural Science Foundation of China (81025006 (Z.Y.), 81170883 (Z.Y.) and the Department of Science and Technology of Sichuan Province, China (2014SZ0169 (Z.Y.) and 2012SZ0219 (Z.Y.)). The Singapore Chinese Health Study was founded by NUS-HUJ CREATE Programme of the National Research Foundation, Singapore (Project No. 370062002), the National Medical Research Council (NMRC/1270/2010), Singapore, and the National Institutes of Health, USA (NCI RO1 CA55069, R35 CA53890, R01 CA80205 and R01 CA144034). C.-Y.C. is supported by an award from NMRC (CSA/033/2012), Singapore. The Singapore Tissue Network and the Tissue Repository of National University Health System provided services for DNA sample storage in Singapore. The Genome Institute of Singapore, Agency for Science, Technology and Research, Singapore provided services for genotyping.

Author contributions

C.-Y.C., K.Y., L.J.C., J.A., K.-H.P., C.P.P., N.Y., T.Y.W. and C.C.K. designed the study. C.-Y.C., C.M.G.C., M.M., P.D.C., I.Y.Y., A.L., R.M., A.H.K., S.Y.L., D.W., C.M.G.C., B.K.L., Y.S., H.N., Y.A.-K., N.G., A.T., K.M., S.Y., Y.S., H.I., T.I., S.H., T.Y.Y.L., H.C., S.T., X.D., F.W., P.Z., B.Z., J.S., J.-M.Y., W.P.K., R.M.v.D., Y.F., N.W., G.S.W.T., S.J.P., M.B., L.G., T.N., P.M., P.Z., S.-M.S., M.O., T.M., Y.K., S.J.W., H.C., H.-G.Y., J.Y.S., D.H.P., I.T.K., W.C., M.S., S.-J.L., H.W.K., J.E.L., C.K.H., T.H.L., S.-K.Y., T.A. and W.T.Y. gathered clinical data. J.P., S.D., I.N., Y.A.-K., F.M., P.O.S.T., F.L., X.Z., Y.S., B.G., R.D., Y.L., M.L.H., J.N.F., C.H.W., X.X., Jinlong Liang, J.M., X.J., Y.L., Jianjun Liu, K.S., E.N.V., J.X.B., Y.X.Z. and C.C.K. generated genetic data. C.-Y.C., K.Y., L.J.C., J.A., Lulin Huang, Lvzhen Huang, K.S.S., P.C., Jiemin Liao, P.G.O., Y.Y.T. and C.C.K. analysed the data. C.-Y.C., K.Y., L.J.C., J.A., Lulin Huang, Lvzhen Huang, E.S.T., X.X.L., Z.Y., K.H.P., C.P.P, N.Y., T.Y.W. and C.C.K. interpreted the data. C.-Y.C., K.Y., L.J.C., J.A., E.S.T., T.Y.W. and C.C.K. drafted the paper. All the authors contributed to revision of the paper.

Additional information

Supplementary Information accompanies this paper at http://www.nature.com/naturecommunications

Competing financial interests: The authors declare no competing financial interests.

Reprints and permission information is available online at http://npg.nature.com/reprintsandpermissions/

How to cite this article: Cheng, C.-Y. *et al.* New loci and coding variants confer risk for age-related macular degeneration in East Asians. *Nat. Commun.* 6:6063 doi: 10.1038/ncomms7063 (2015).

Association of Focal Choroidal Excavation With Age-Related Macular Degeneration

Yoshimasa Kuroda,[1] Akitaka Tsujikawa,[1] Sotaro Ooto,[1] Kenji Yamashiro,[1] Akio Oishi,[1] Hideo Nakanishi,[1] Kyoko Kumagai,[1] Masayuki Hata,[1] Shigeta Arichika,[1] Abdallah A. Ellabban,[1,2] and Nagahisa Yoshimura[1]

[1]Department of Ophthalmology and Visual Sciences, Kyoto University Graduate School of Medicine, Kyoto, Japan
[2]Department of Ophthalmology, Suez Canal University, Faculty of Medicine, Ismailia, Egypt

Correspondence: Akitaka Tsujikawa, Department of Ophthalmology and Visual Sciences, Kyoto University Graduate School of Medicine, Sakyo-ku, Kyoto 606-8507, Japan; tujikawa@kuhp.kyoto-u.ac.jp.

Submitted: May 2, 2014
Accepted: August 24, 2014

Citation: Kuroda Y, Tsujikawa A, Ooto S, et al. Association of focal choroidal excavation with age-related macular degeneration. *Invest Ophthalmol Vis Sci.* 2014;55:6046–6054. DOI: 10.1167/iovs.14-14723

Purpose. To study the prevalence, tomographic features, and clinical characteristics of focal choroidal excavation (FCE) in eyes with exudative age-related macular degeneration (AMD).

Methods. We examined 243 consecutive eyes with exudative AMD with a prototype swept-source optical coherence tomography (OCT) system. Three-dimensional images of the macular area, covering 6 × 6 mm^2, were reconstructed by segmentation of the outer surface of the retinal pigment epithelium.

Results. Three-dimensional swept-source OCT revealed 15 excavations in 12 eyes (4.9%); 10 had a single excavation and 2 had multiple excavations (2 and 3 excavations, respectively). In multiaveraged scans, unusual choroidal tissue was found beneath 5 excavations, bridging the excavation with the outer choroidal boundary. Additionally, the suprachoroidal space was observed beneath 7 excavations—the outer choroidal boundary appeared to be pulled inward by this bridging tissue. In 9 excavations, color fundus photographs showed pigmentary disturbance. Fourteen excavations (93.3%) were located within or adjacent to the choroidal neovascularization area. Compared with eyes without FCE, in eyes with FCE, the mean age was significantly higher ($P = 0.040$) and mean visual acuity was significantly better ($P = 0.014$). In addition, polypoidal lesions were observed in 8 of 12 eyes with FCE, but they appeared to have a limited effect on either the rate of FCE ($P = 0.44$) or the clinical characteristics of the eyes.

Conclusions. While FCE may be partially related to the choroidal neovascularization associated with exudative AMD, other factors may also influence this association.

Keywords: focal choroidal excavation, exudative age-related macular degeneration, swept-source optical coherence tomography

Focal choroidal excavation (FCE) is a newly recognized clinical entity. It was first identified in 2006 by Jampol et al.[1] by using time-domain optical coherence tomography (OCT). Focal choroidal excavation is characterized by an intrachoroidal concavity in the macula, without posterior staphyloma or scleral ectasia. Subsequent studies using spectral-domain OCT have elucidated the clinical and morphological characteristics of FCE.[2–12] Initially, FCE was considered a stable choroidal abnormality and an incidental finding in patients with metamorphopsia or blurred vision.[10]

Recently, it has been suggested that FCE may form the basis of choroidal neovascular diseases. Kobayashi and associates[7] reported a case of FCE accompanied by polypoidal choroidal vasculopathy (PCV). Xu et al.[12] found choroidal neovascularization (CNV) at the bottom or slope of the excavations in 15 eyes (12 patients). In addition, Lee and Lee[9] studied eight patients, aged over 50 years, who had CNV around the excavations. In older people, age-related macular degeneration (AMD) is the most common choroidal neovascular disease.[13,14] On the basis of these previous reports, we hypothesized that FCE may be involved in the development of CNV associated with exudative AMD. To date, however, because these reports are single case reports or small case series, the prevalence and clinical characteristics of complications associated with FCE remain unknown.

In recent years, swept-source OCT with a longer-wavelength light source has provided better views of the choroid because of improved light penetration into the choroid.[15–19] In addition, the tunable laser source of swept-source OCT shows lower signal decay with increasing depth, further improving visibility of the choroidal features. Furthermore, the high imaging speed allows for dense scanning and subsequent three-dimensional (3-D) image reconstruction of the posterior pole. In the current study, we prospectively examined the macular area in consecutive eyes with exudative AMD by using 1-μm-wavelength swept-source OCT to study the prevalence and clinical and tomographic features of FCE and the possible association of FCE and CNV with exudative AMD.

Methods

The Ethics Committee at Kyoto University Graduate School of Medicine approved this prospective study, which was conducted in accordance with the tenets of the Declaration of Helsinki.

Written informed consent was obtained from each subject before any study procedures or examinations were performed.

We used 3-D swept-source OCT imaging to prospectively examine 243 eyes of 217 consecutive exudative AMD patients who presented to the macula clinic at Kyoto University Hospital between October 2010 and March 2013. All the study subjects were Japanese. They underwent a comprehensive ocular examination, including autorefractometry, best-corrected visual acuity measurement with a Landolt C chart, slit-lamp biomicroscopy, intraocular pressure measurement, fundus photography (TRC-NW8F; Topcon Corp., Tokyo, Japan), 3-D swept-source OCT imaging with a prototype system (Topcon Corp.), and simultaneous fluorescein angiography (FA) and indocyanine green angiography (ICGA) by using the Spectralis HRA+OCT (Heidelberg Engineering, Heidelberg, Germany). Several patients underwent an additional OCT scan using RS-3000 OCT (Nidek, Gamagori, Japan) or Spectralis OCT (Heidelberg Engineering). The exclusion criteria included other macular abnormalities, for example, pathologic myopia, angioid streaks, retinal angiomatous proliferation, idiopathic CNV, other secondary CNV, intraocular inflammation, history of ocular trauma, poor image due to a thick subretinal hemorrhage, or history of vitrectomy.

The prototype swept-source OCT used in the current study has been reported previously.[20,21] It uses a light source of a wavelength-sweeping laser centered at 1050 nm with a tuning range of 100 nm. This system has a scanning speed of 100,000 A-scans per second and a scan window depth of 2.6 mm. The axial and transverse resolutions are 8 μm and 20 μm in tissue, respectively. The optical power incident on the cornea is less than 1 mW, which meets the safety requirements for this laser class according to the American National Standards Institute.

Swept-source OCT examinations were performed by trained examiners after pupil dilation. In each subject, 3-D volumetric scans were acquired in 0.8 seconds, with 512 (horizontal) × 128 (vertical) A-scans (total, 65,536 axial scans/volume). Each 3-D volumetric scan consisted of 128 B-scans and covered an area of 6 × 6 mm^2, centered on the fovea. Pupil centration during the scan was achieved by using an internal fixation target and confirmed by a built-in camera within the swept-source OCT system. Owing to the high speed and invisible-wavelength scanning light, eye movements during the 3-D image acquisition were minimal. To decrease speckle noise, each image was denoised by the weighted moving average of three consecutive original B-scans.

On OCT, focal excavation was identified when Bruch's membrane line was excavated into the choroid focally, without any history of trauma, infection, posterior uveitis, or choroidal vascular disease. The excavations were divided into two types: conforming and nonconforming. Conforming excavations implied that the photoreceptor tips were attached to the retinal pigment epithelium (RPE). In nonconforming excavations, the photoreceptor tips were detached from the RPE.[4]

In eyes with FCE, 3-D topographical images were reconstructed from the OCT scans, by segmentation of the line of the outer surface of the RPE, to highlight the shape of the excavation. In each B-scan, the outer surface of the RPE line was automatically determined by the software, and manual corrections were made as necessary using the built-in segmentation-modifying tool. The excavation depth and width were measured manually from the 3-D dataset, using the scan that showed the greatest dimensions.

Polypoidal choroidal vasculopathy was diagnosed based on ICGA, which showed branching vascular networks that terminated in polypoidal lesions.[22,23] In the current study, the angiographic features in the area of the excavations were examined. Additionally, the correlations between the locations of the excavations, the area of CNV, and areas of choroidal vascular hyperpermeability in ICGA were analyzed. Choroidal vascular hyperpermeability was defined as multifocal areas of hyperfluorescence with blurred margins within the choroid in the mid to late phase of ICGA.[24]

The retinal and choroidal thicknesses at the center of the fovea were manually measured with a built-in caliber tool. Retinal thickness was defined as the distance between the vitreoretinal interface and the outer border of the RPE, and choroidal thickness was defined as the distance between the line corresponding to the Bruch's membrane beneath the RPE and the chorioscleral interface. When the excavation was located within the foveal center, choroidal thickness was measured as the distance between the supposed line of Bruch's membrane and the chorioscleral interface.

All values are presented as mean ± standard deviation. The measured visual acuity was converted to the logarithm of the minimum angle of resolution (logMAR) for statistical analyses. Mann-Whitney tests were used to compare numerical variable means, and Fisher's exact tests were used to compare the distribution of categorical variables. Statistical significance was indicated when the P value was less than 0.05.

Results

Two hundred forty-three eyes of 217 consecutive patients with exudative AMD were examined by swept-source OCT. Fluorescein angiography showed CNV within the macular area in all the eyes, and ICGA revealed polypoidal lesions in 136 eyes. Of the 243 eyes with exudative AMD, 12 (4.9%) were found to have FCE. Of the 12 eyes with FCE, polypoidal lesions were seen in 8 eyes. Focal choroidal excavations were found in 5.9% of eyes with PCV and in 3.7% of eyes with AMD without polypoidal lesions. Table 1 shows the clinical characteristics of eyes with FCE associated with AMD. The mean age of eyes with FCE was 69.7 ± 9.2 years (range, 57–83 years). Five eyes were myopic, and the mean spherical equivalent was –0.63 ± 3.25 diopters. The mean foveal retinal thickness was 255.7 ± 124.8 μm (range, 111–588 μm), and the mean foveal choroidal thickness was 257.5 ± 92.3 μm (range, 146–467 μm).

The 3-D scanning protocol of swept-source OCT allowed the detection of excavations in the macular area and visualization of their morphology (Fig. 1). Of 12 eyes with FCE, 10 had a single excavation and 2 had multiple excavations (2 and 3 excavations, respectively). Six excavations were classified into the conforming type, and nine were of the nonconforming type. The mean depth of the excavations was 53.3 ± 19.6 μm (range, 22–106 μm), and the mean width of the excavations was 799.7 ± 404.5 μm (range, 388–1986 μm). The inner retinal layers appeared normal, and even when the excavation was located subfoveally, the foveal contour remained nearly well preserved. In 13 (86.6%) excavations, the line of the external limiting membrane was preserved. In 3 (20.0%) excavations, the line forming the junction between the inner and outer segments of the photoreceptors remained continuous. The RPE line was intact in all the eyes, despite some thinning or attenuation (Table 2).

Swept-source OCT also allowed visualization of the choroidal structures. Multiaveraged scans often showed an inner choroidal layer with medium-diameter blood vessels and an outermost choroidal layer with larger-diameter blood vessels. In five excavations (33.3%), unusual choroidal tissue devoid of large vessels was detected beneath the excavation, bridging the bottom of the excavation with the outer choroidal boundary (Fig. 2). In addition, the suprachoroidal space was observed beneath seven excavations (46.7%)—the outer choroidal boundary appeared to be pulled inward by the bridging tissue

Investigative Ophthalmology & Visual Science

Table 1. Clinical Characteristics of Eyes With Focal Choroidal Excavation Associated With Age-Related Macular Degeneration

Patient	Age, y	Sex	Visual Acuity‡	Refractive Error Spherical Equivalent, Diopters	Excavation				FRT, µm	FChT, µm	Previous Treatment	Duration of Follow-Up With OCT Examination, mo
					Location	Type	Depth, µm	Width, µm				
1	83	F	0.08	0	Extrafovea	Conforming	45	465	111	205	PC	65
2	57	M	1.0	−1.25	Extrafovea	Nonconforming	50	540	174	327		2
3	83	M	1.2	3.25	Extrafovea	Nonconforming	67	865	258	340		3
4*	58	M	1.5	−4.0	Extrafovea	Conforming	77	1033	216	155	IVR	18
					Extrafovea	Conforming	51	836				
					Extrafovea	Conforming	22	388				
5	77	M	0.2	2.5	Extrafovea	Conforming	54	714	588	321	0	1
6	61	M	1.5	1.0	Extrafovea	Nonconforming	49	681	234	467	0	60
7	75	M	0.9	5.0	Subfovea	Conforming	38	463	173	146	PDT	60
8	69	M	1.5	−3.0	Extrafovea	Nonconforming	38	1080	304	190	0	20
9	73	M	0.7	−0.25	Subfovea	Nonconforming	38	583	255	223	0	29
10†	67	M	0.7	−6.5	Extrafovea	Nonconforming	106	1997	372	219	0	7
					Extrafovea	Nonconforming	49	404				
11	60	F	0.7	0.5	Subfovea	Nonconforming	58	1200	179	271	0	61
12	73	M	0.8	2.0	Extrafovea	Nonconforming	57	1121	204	226	0	53

F, female; M, male; FRT, foveal retinal thickness; FChT, foveal choroidal thickness; PC, photocoagulation; IVR, intravitreal injections of ranibizumab; PDT, photodynamic therapy.

* Patient 4 had three excavations.

† Patient 10 had two excavations.

‡ Landolt visual acuity.

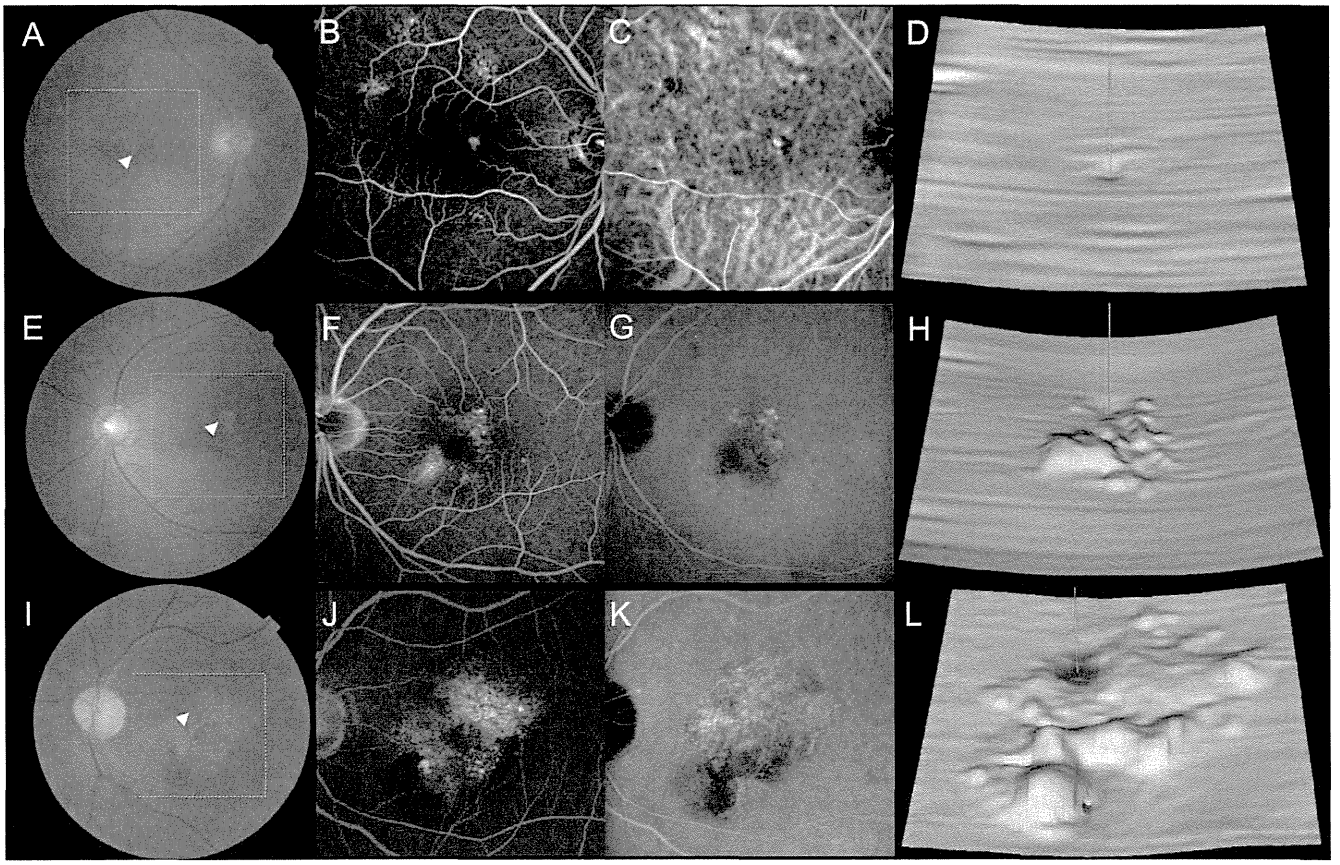

Figure 1. Three eyes with exudative age-related macular degeneration with focal choroidal excavation examined with swept-source optical coherence tomography (OCT). (**A–D**) Patient 7, (**E–H**) patient 8, and (**I–L**) patient 12. (**A**, **E**, **I**) Focal excavations were detected in fundus photographs as pigmentary disturbances (*arrowheads*). (**B**, **F**, **J**) Fluorescein angiogram. (**C**, **G**, **K**) Indocyanine green angiogram showing choroidal neovascularization. (**D**, **H**, **L**) Reconstructed three-dimensional OCT images (*dashed yellow squares* in fundus photographs) of the retinal pigment epithelium showing the shape of the excavations. *White bars* indicate the center of the excavations.

Table 2. Angiographic and Tomographic Characteristics of Eyes With and Without Focal Choroidal Excavation Associated With Age-Related Macular Degeneration

		Angiographic Findings				Optical Coherence Tomographic Findings				
Patient	Color Photography Findings	Correlation Between Excavation and Choroidal Neovascularization	Polypoidal Lesions	Choroidal Hyperpermeability	Correlation Between FCE and Choroidal Hyper-permeability	Unusual Choroidal Tissue Below Excavation	Suprachoroidal Space Below Excavation	ELM Band	IS/OS Band	RPE
1	Pigmentary disturbance	Within	−	−	−	−	−	−	−	+
2	Pigmentary disturbance	Within	−	−	−	+	+	+	−	+
3	Atrophy	Outside	−	+	Within	−	−	−	−	+
4	Pigmentary disturbance	Within	−	+	Adjacent	+	+	+	−	+
	Pigmentary disturbance	Within	−	+	Adjacent	−	+	+	−	+
	Pigmentary disturbance	Within	−	+	Adjacent	−	+	+	−	+
5	Hemorrhage	Adjacent	+	+	Within	−	−	+	−	+
6	Physiological	Within	+	−	−	−	−	+	+	+
7	Pigmentary disturbance	Adjacent	+	+	Within	+	−	+	+	+
8	Pigmentary disturbance	Adjacent	+	−	−	−	−	+	+	+
9	Pigmentary disturbance	Within	+	+	Within	+	+	+	−	+
10	Pigmentary disturbance	Within	+	−	−	+	+	+	−	+
	Physiological	Adjacent	+	−	−	−	+	+	−	+
11	Physiological	Within	+	−	−	−	−	+	−	+
12	Physiological	Within	+	−	−	−	−	+	−	+

ELM, external limiting membrane; IS/OS, inner segment/outer segment.

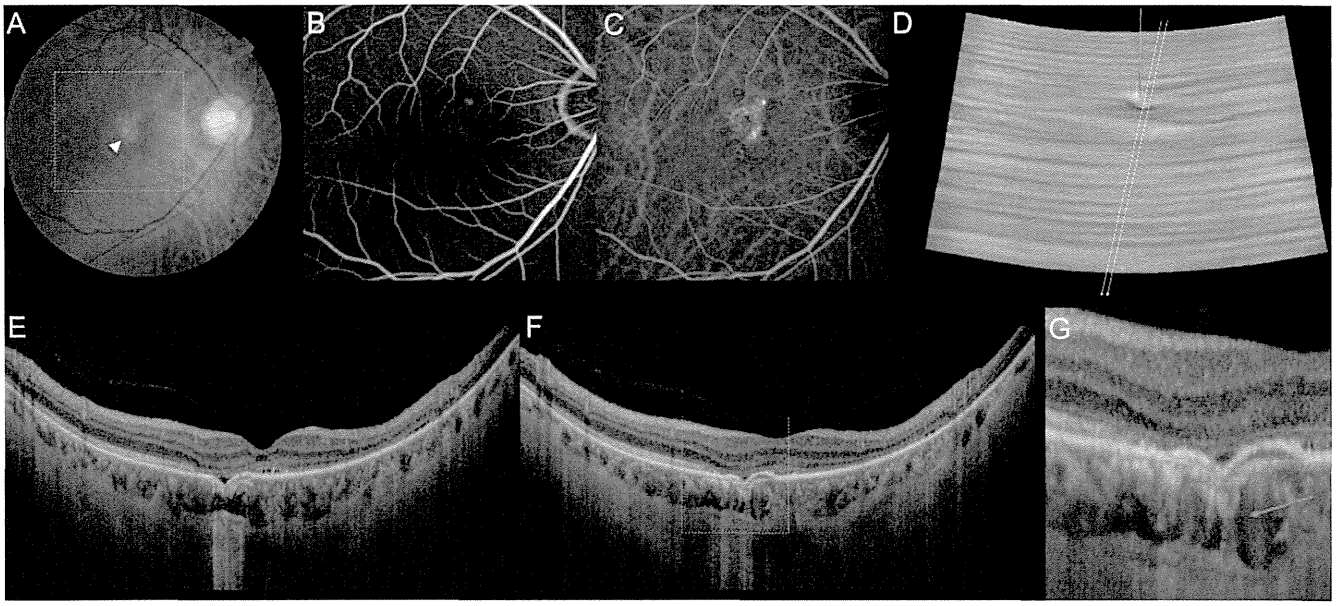

FIGURE 2. Unusual choroidal tissue under the excavation revealed by swept-source optical coherence tomography (OCT). (**A**) Fundus photograph of the right eye of a 57-year-old man with exudative age-related macular degeneration (patient 2). Fundus photograph showing pigmentary disturbance of the retinal pigment epithelium in the area corresponding to the excavation (*white arrowhead*). The *dashed yellow square* outlines the area (6×6 mm^2) scanned by the swept-source OCT. (**B**) Fluorescein angiogram. (**C**) Indocyanine green angiogram showing choroidal neovascularization. (**D**) Image reconstructed by segmentation of the retinal pigment epithelium showing the three-dimensional shape of the excavation. (**E**, **F**) Multiaveraged OCT sections were made along the *long white arrows*, as seen in the three-dimensional image. Vertical OCT sections through the fovea showing a nonconforming focal choroidal excavation. (**G**) Magnified image of the area outlined by the *dashed white square*. Unusual choroidal tissue (*red arrow*) is seen bridging the bottom of the excavation and the outer choroidal boundary.

(Fig. 3). The chorioscleral interface was smooth, without scleral outpouching in all the eyes.

Table 2 shows funduscopic and angiographic characteristic of eyes with FCE associated with AMD. In 9 excavations (60.0%), color fundus photographs showed pigmentary disturbances. Fluorescein angiography and/or ICGA revealed CNV in all the eyes. Although four patients (4 eyes) did not receive ICGA because of iodine allergy, all of 12 eyes with FCE were examined with ICGA. Of 15 excavations, 14 (93.3%) were located within or adjacent to the area of CNV (Fig. 4). Five eyes (41.7%) showed choroidal hyperpermeability in the mid or late phase of ICGA. In these eyes, all 7 excavations (46.7%) were seen within or adjacent to the areas of choroidal hyperpermeability.

In the current study, the mean follow-up period was 31.6 ± 26.3 months (range, 1–65 months). During the follow-up period, eight eyes received intravitreal injections of ranibizumab and one received photodynamic therapy combined with ranibizumab. One eye was not followed after the initial injection of ranibizumab; the mean number of injections in the remaining seven eyes was 5.1 ± 2.1 (range, 3–9). In five of these seven eyes, no exudative changes were observed at the final follow-up examination. Nonconforming excavations changed to the conforming type when the eyes responded to treatment for CNV. In the five eyes that were followed for more than 4 years, no changes in the size or shape of the excavations were detected (Supplementary Fig. S1).

Comparisons of parametric data of eyes with AMD and FCE with those of eyes with AMD and without FCE are shown in Table 3. There were no significant differences in sex distribution, refractive error, and the foveal retinal or choroidal thicknesses between the two groups. Compared with eyes without FCE, in eyes with FCE, the mean age was significantly higher ($P = 0.040$) and the mean visual acuity was significantly better ($P = 0.014$). In addition, we found that the presence of polypoidal lesions had a limited effect on either the rate of FCE ($P = 0.44$) or the clinical characteristics of the eyes.

DISCUSSION

It remains unknown whether FCE is a congenital choroidal malformation or an acquired insult. Kumano et al.[8] speculated that the excavation is caused by outward traction due to choroidal vascular abnormalities resulting from developmental failure in the embryo. In eyes with central serous chorioretinopathy (CSC), Ellabban et al.[25] recently showed unusual choroidal tissue beneath the excavation that bridged the bottom of the excavation and the outer choroidal boundary and could possibly produce the excavation. In the current study, we found similar choroidal tissue beneath five excavations. In addition, the suprachoroidal space was observed beneath seven excavations—it appeared as if the outer choroidal boundary was pulled inward by this bridging tissue. In addition, the shape of most excavations was irregular and often pointed outward. This irregular shape could be attributed to the presence of outward traction on the RPE.

Initially, FCE was thought to be a quiescent choroidal abnormality with good visual prognosis. It was later found that FCE is associated with vision-threatening complications, including CNV and polypoidal lesions.[7,9] In the current study, 14 excavations were located within or adjacent to the area of CNV. In a recent study, Xu et al.[12] reported CNV that was present at the bottom or slope of the excavation in 15 eyes. It is unclear whether CNV developed from the excavation or whether CNV contributed to the formation of the excavation. Because FCE alone rarely causes serious visual symptoms, most of our patients presented at the clinic immediately after noticing CNV-associated visual symptoms. In addition, in a recent study of eyes in which CNV developed from FCE during

Investigative Ophthalmology & Visual Science

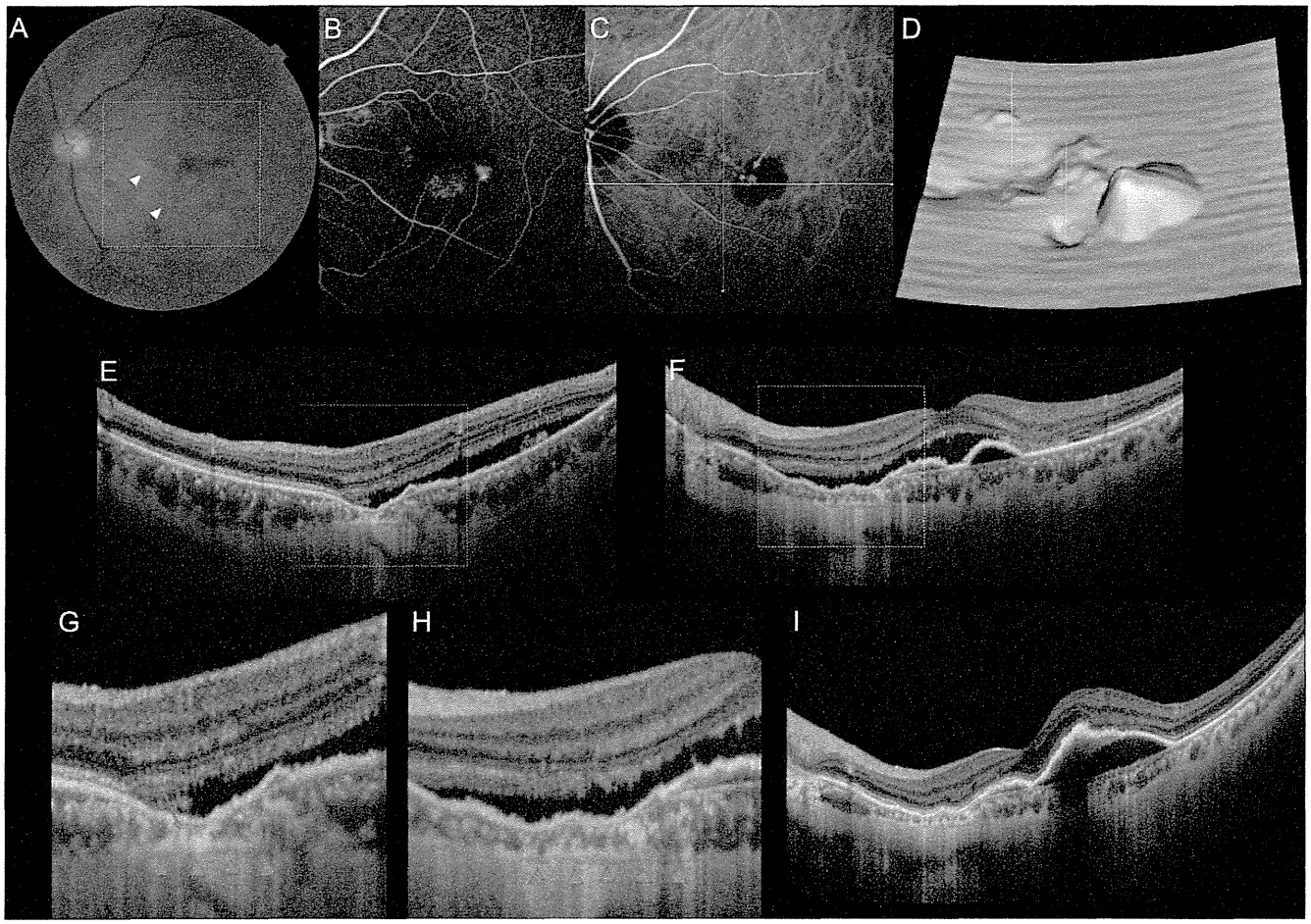

FIGURE 3. Suprachoroidal space beneath the excavation revealed by swept-source optical coherence tomography (OCT). (**A**) Fundus photograph of the left eye of a 67-year-old man with polypoidal choroidal vasculopathy (patient 10) showing pigmentary disturbances in the areas corresponding to the excavations (*white arrowheads*). The *dashed yellow square* outlines the area (6×6 mm^2) scanned by the swept-source OCT. (**B**) Fluorescein angiogram showing occult choroidal neovascularization. (**C**) Indocyanine green angiogram (ICGA) showing polypoidal lesions (*red arrow*). (**D**) Image reconstructed by segmentation of the retinal pigment epithelium showing the three-dimensional shape of the excavation. *White bars* indicate the center of the excavations. (**E**) Vertical and (**F**) horizontal multiaveraged OCT sections along the *long white arrows* on ICGA showing nonconforming excavations. (**G**, **H**) Magnified images of the areas outlined by the *dashed white square*. Beneath the focal choroidal excavation, unusual choroidal tissue (*red arrow*) is seen bridging the bottom of the excavation and the outer choroidal boundary. The suprachoroidal space (*arrowheads*) is seen below the excavation. (**I**) Horizontal OCT scans obtained after six monthly intravitreal injections of ranibizumab: The excavation changed from the nonconforming to conforming type with the resolution of the serous detachment. There were no remarkable changes in the dimensions or the shape of the excavation during the follow-up period.

the follow-up period, CNV was found to develop from choroidal excavations.

The mechanism underlying the association of these excavations with CNV remains unclear. Obata et al.[10] reported that excavations may lead to aberrant choroidal circulation. In the current study, a few eyes with FCE showed no large choroidal vessels beneath the excavations. Focal choroidal ischemia may be involved in the development of CNV.[26–29] In the current study, color fundus photographs showed pigmentary disturbances in nine excavations. Focal damage of the RPE and Bruch's membrane due to the excavation may contribute to the development of CNV.[30] In a recent report of CNV associated with FCE in younger patients, all CNV showed classic appearance in FA. In addition, two recent case series reported a good response to ranibizumab or bevacizumab in younger patients with CNV associated with FCE. Notably, Xu et al.[12] reported that in 13 of 15 eyes with CNV, CNV regressed with a single injection of ranibizumab. These angiographic characteristics and treatment responses are not found in exudative AMD but are rather typical of secondary CNV.[31,32] In younger patients, the pathogenesis of CNV associated with FCE would be different from that of CNV associated with exudative AMD.

In contrast, in another report of CNV associated with FCE, six of eight patients under the age of 50 had type 2 CNV, whereas seven of eight patients over the age of 50 had type 1 CNV.[9] Similarly, 11 of our patients, all of whom were more than 50 years old, had PCV or type 1 CNV that was located under the RPE. Kobayashi et al.[7] have reported the limited efficacy of ranibizumab in PCV associated with FCE, and our patients needed repeated injections of ranibizumab. Because exudative AMD is the most common choroidal neovascular disease in people over the age of 50,[13,14] we speculate that some cases of CNV seen in eyes with exudative AMD might be associated with FCE. However, because FCE was seen in 12 eyes (4.9%) with exudative AMD, its role may be limited. The pathogenesis of CNV that develops around the excavation in older subjects may be different from that in younger subjects.

Margolis et al.[4] and Katome et al.[6] reported that FCE is common in eyes with a thicker choroid. Ellabban et al.[25]

Investigative Ophthalmology & Visual Science

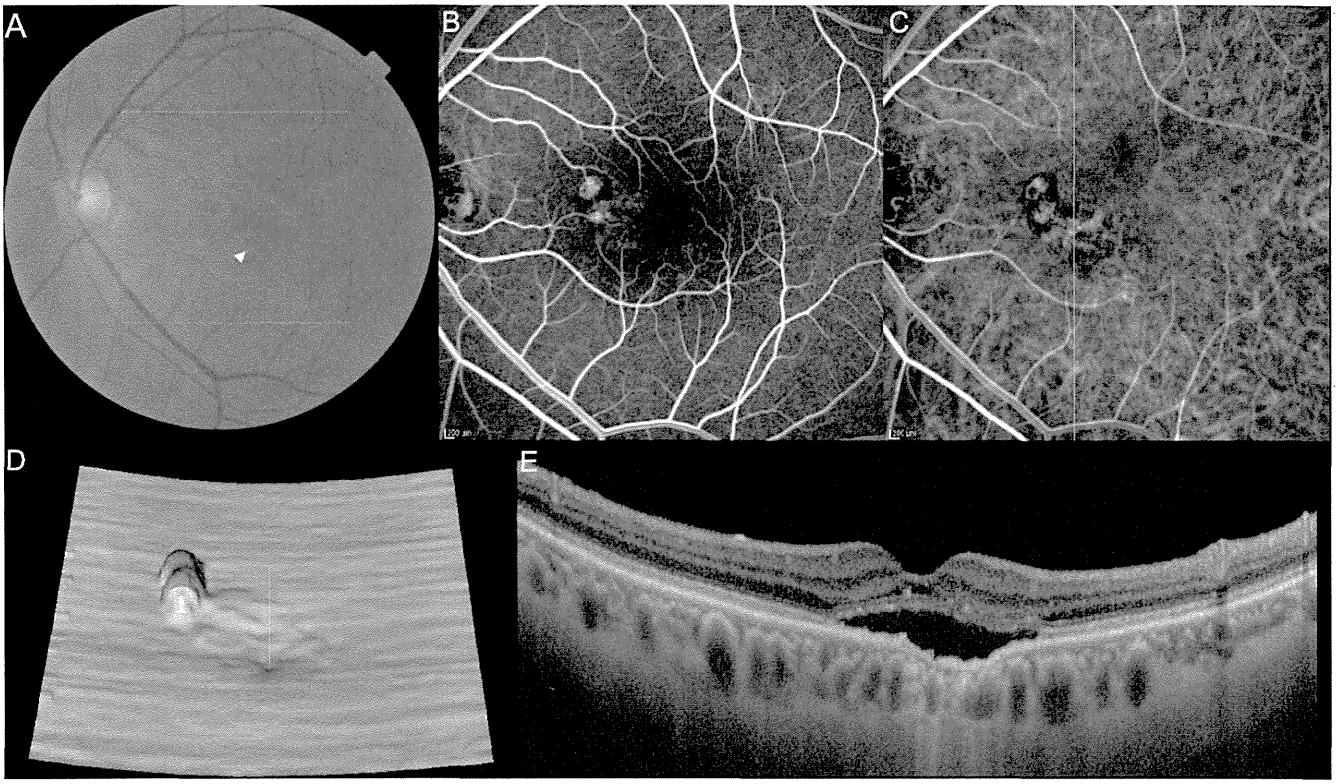

FIGURE 4. A focal excavation consistent with a branching vascular network associated with polypoidal choroidal vasculopathy. (**A**) Fundus photograph of the left eye of a 73-year-old man with polypoidal choroidal vasculopathy showing pigmentary disturbance in the areas corresponding to the excavations (*white arrowhead*) (patient 9). (**B**) Fluorescein angiogram showing occult choroidal neovascularization. (**C**) Indocyanine green angiogram (ICGA) showing a branching vascular network terminating in polypoidal lesions (*red arrow*). (**D**) Three-dimensional image reconstructed by segmentation of the retinal pigment epithelium showing the shape of the excavation (*white bar*). (**E**) Vertical section of a swept-source optical coherence tomography image along the *white arrow* in the ICGA showing a noncomforming excavation with serous retinal detachment. The excavation is consistent with a branching vascular network.

reported that the choroidal thickness in CSC eyes with FCE was significantly thicker than that in normal eyes but thinner than that in CSC eyes without FCE. The reason for this difference is unclear. Recent OCT image analysis revealed choroidal thinning in eyes with exudative AMD, compared with PCV.[33,34] In our patients with FCE, subfoveal choroidal thickness in eyes with PCV was similar to that in eyes with exudative AMD without polypoidal lesions. Jirarattanasopa et al.[35] reported local choroidal thickening in areas of choroidal vascular hyperpermeability. In our patients, three of four eyes with exudative AMD and three of eight eyes with PCV had choroidal vascular hyperpermeability. The higher rate of choroidal vascular hyperpermeability in eyes with exudative AMD may account for our finding of similar choroidal thickness.

Previous reports showed that most eyes with FCE are myopic. However, in our study, only five eyes with FCE associated with exudative AMD were myopic. The reason for this observation is unknown. However, in a previous report by Xu et al.,[12] 50% of eyes with FCE that developed CNV were nonmyopic. While FCEs were often seen in myopic eyes, CNV is likely to develop in less myopic eyes with FCE.

TABLE 3. Eyes With and Without Focal Choroidal Excavation Associated With Polypoidal Lesions

	With FCE			Without FCE			
	Total	Without Polypoidal Lesions	With Polypoidal Lesions	Total	Without Polypoidal Lesions	With Polypoidal Lesions	*P* Value*
N, eyes	12	4	8	231	103	128	
Sex, male/female	10/2	3/1	7/1	147/84	65/38	82/46	0.138†
Age, y	69.7 ± 9.2	70.3 ± 14.7	69.4 ± 6.3	75.3 ± 8.0	76.0 ± 8.1	74.7 ± 7.9	0.040‡
Refractive error, diopters	−0.63 ± 3.25	−0.50 ± 3.01	0.16 ± 3.54	0.84 ± 2.02	1.01 ± 2.20	0.70 ± 1.87	0.371‡
Visual acuity, logMAR	0.15 ± 0.38	0.21 ± 0.60	0.12 ± 0.27	0.41 ± 0.44	0.48 ± 0.46	0.36 ± 0.42	0.014‡
Foveal retinal thickness, μm	255.7 ± 124.8	189.8 ± 62.7	288.6 ± 138.1	261.9 ± 148.8	286.7 ± 182.0	242.0 ± 112.2	0.951‡
Foveal choroidal thickness, μm	257.5 ± 92.3	256.8 ± 91.1	257.9 ± 99.1	232.0 ± 96.5	232.9 ± 97.8	231.3 ± 95.8	0.414‡

* Compared with eyes with and without FCE.
† Fisher's exact test.
‡ Mann-Whitney test.

The current study had several limitations. First, because the number of eyes with FCE was small, the clinical characteristics could not be elucidated fully. Second, all subjects were Asian, and it is possible that the prevalence of FCE is different among other ethnicities. Third, all of our patients had both CNV and FCE upon initial examination because FCE alone rarely causes serious visual symptoms. The current study could not provide information about the condition before the development of CNV. In addition, in the absence of normal control eyes without exudative AMD, a true association between AMD and FCE cannot be established.

In summary, taking into consideration our findings as well as those of previous studies, we hypothesized that the pathogenesis of neovascular complications was induced by FCE involved with outward traction by connective choroidal tissue, possibly resulting from embryonic developmental failure. In general, FCE is a stable condition with minimal symptoms. In some younger patients with FCE, focal damage of the RPE and Bruch's membrane due to the excavation and focal choroidal ischemia may lead to the development of CNV. The clinical characteristics of these CNV are different from those of typical exudative AMD, and they are rather similar to those of secondary CNV. Some older patients with FCE may develop CNV or polypoidal lesions. Although FCE might be partly related to development of CNV associated with exudative AMD, its role appears limited to some eyes.

Acknowledgments

Supported, in part, by the Japan Society for the Promotion of Science (JSPS), Tokyo, Japan (Grant-in-Aid for Scientific Research 21592256) and the Japan National Society for the Prevention of Blindness, Tokyo, Japan.

Disclosure: **Y. Kuroda**, None; **A. Tsujikawa**, Pfizer (F); **S. Ooto**, None; **K. Yamashiro**, None; **A. Oishi**, None; **H. Nakanishi**, None; **K. Kumagai**, None; **M. Hata**, None; **S. Arichika**, None; **A.A. Ellabban**, None; **N. Yoshimura**, Topcon Corp. (F), Nidek (F, C), Canon (F)

References

1. Jampol LM, Shankle J, Schroeder R, Tornambe P, Spaide RF, Hee MR. Diagnostic and therapeutic challenges. *Retina*. 2006;26: 1072-1076.
2. Abe S, Yamamoto T, Kirii E, Yamashita H. Cup-shaped choroidal excavation detected by optical coherence tomography: a case report. *Retin Cases Brief Rep*. 2010;4:373-376.
3. Wakabayashi Y, Nishimura A, Higashide T, Ijiri S, Sugiyama K. Unilateral choroidal excavation in the macula detected by spectral-domain optical coherence tomography. *Acta Ophthalmol*. 2010;88:e87-e91.
4. Margolis R, Mukkamala SK, Jampol LM, et al. The expanded spectrum of focal choroidal excavation. *Arch Ophthalmol*. 2011;129:1320-1325.
5. Chen JC, Gupta RR. A case of multiple focal choroidal excavations. *Can J Ophthalmol*. 2012;47:e56-e58.
6. Katome T, Mitamura Y, Hotta F, Niki M, Naito T. Two cases of focal choroidal excavation detected by spectral-domain optical coherence tomography. *Case Rep Ophthalmol*. 2012;3:96-103.
7. Kobayashi W, Abe T, Tamai H, Nakazawa T. Choroidal excavation with polypoidal choroidal vasculopathy: a case report. *Clin Ophthalmol*. 2012;6:1373-1376.
8. Kumano Y, Nagai H, Enaida H, Ueno A, Matsui T. Symptomatic and morphological differences between choroidal excavations. *Optom Vis Sci*. 2013;90:e110-e118.
9. Lee JH, Lee WK. Choroidal neovascularization associated with focal choroidal excavation. *Am J Ophthalmol*. 2014;157:710-718, e711.
10. Obata R, Takahashi H, Ueta T, Yuda K, Kure K, Yanagi Y. Tomographic and angiographic characteristics of eyes with macular focal choroidal excavation. *Retina*. 2013;33:1201-1210.
11. Say EA, Jani PD, Appenzeller MF, Houghton OM. Focal choroidal excavation associated with polypoidal choroidal vasculopathy. *Ophthalmic Surg Lasers Imaging Retina*. 2013; 44:409-411.
12. Xu H, Zeng F, Shi D, Sun X, Chen X, Bai Y. Focal choroidal excavation complicated by choroidal neovascularization. *Ophthalmology*. 2014;121:246-250.
13. Bressler NM. Age-related macular degeneration is the leading cause of blindness. *JAMA*. 2004;291:1900-1901.
14. Friedman DS, O'Colmain B, Munoz B, et al. Prevalence of age-related macular degeneration in the United States. *Arch Ophthalmol*. 2004;122:564-572.
15. Ikuno Y, Kawaguchi K, Nouchi T, Yasuno Y. Choroidal thickness in healthy Japanese subjects. *Invest Ophthalmol Vis Sci*. 2010;51:2173-2176.
16. Yasuno Y, Hong Y, Makita S, et al. In vivo high-contrast imaging of deep posterior eye by 1-μm swept source optical coherence tomography and scattering optical coherence angiography. *Opt Express*. 2007;15:6121-6139.
17. de Bruin DM, Burnes DL, Loewenstein J, et al. In vivo three-dimensional imaging of neovascular age-related macular degeneration using optical frequency domain imaging at 1050 nm. *Invest Ophthalmol Vis Sci*. 2008;49:4545-4552.
18. Esmaeelpour M, Povazay B, Hermann B, et al. Three-dimensional 1060-nm OCT: choroidal thickness maps in normal subjects and improved posterior segment visualization in cataract patients. *Invest Ophthalmol Vis Sci*. 2010;51:5260-5266.
19. Ferrara D, Mohler KJ, Waheed N, et al. En face enhanced-depth swept-source optical coherence tomography features of chronic central serous chorioretinopathy. *Ophthalmology*. 2014;121:719-726.
20. Hirata M, Tsujikawa A, Matsumoto A, et al. Macular choroidal thickness and volume in normal subjects measured by swept-source optical coherence tomography. *Invest Ophthalmol Vis Sci*. 2011;52:4971-4978.
21. Ellabban AA, Tsujikawa A, Matsumoto A, et al. Macular choroidal thickness and volume in eyes with angioid streaks measured by swept source optical coherence tomography. *Am J Ophthalmol*. 2012;153:1133-1143, e1131.
22. Spaide RF, Yannuzzi LA, Slakter JS, Sorenson J, Orlach DA. Indocyanine green videoangiography of idiopathic polypoidal choroidal vasculopathy. *Retina*. 1995;15:100-110.
23. Maruko I, Iida T, Saito M, Nagayama D, Saito K. Clinical characteristics of exudative age-related macular degeneration in Japanese patients. *Am J Ophthalmol*. 2007;144:15-22.
24. Sasahara M, Tsujikawa A, Musashi K, et al. Polypoidal choroidal vasculopathy with choroidal vascular hyperpermeability. *Am J Ophthalmol*. 2006;142:601-607.
25. Ellabban AA, Tsujikawa A, Ooto S, et al. Focal choroidal excavation in eyes with central serous chorioretinopathy. *Am J Ophthalmol*. 2013;156:673-683.
26. Pauleikhoff D, Spital G, Radermacher M, Brumm GA, Lommatzsch A, Bird AC. A fluorescein and indocyanine green angiographic study of choriocapillaris in age-related macular disease. *Arch Ophthalmol*. 1999;117:1353-1358.
27. Grunwald JE, Metelitsina TI, Dupont JC, Ying GS, Maguire MG. Reduced foveolar choroidal blood flow in eyes with increasing AMD severity. *Invest Ophthalmol Vis Sci*. 2005;46:1033-1038.

28. Metelitsina TI, Grunwald JE, DuPont JC, Ying GS, Brucker AJ, Dunaief JL. Foveolar choroidal circulation and choroidal neovascularization in age-related macular degeneration. *Invest Ophthalmol Vis Sci.* 2008;49:358–363.
29. Wakabayashi T, Ikuno Y. Choroidal filling delay in choroidal neovascularisation due to pathological myopia. *Br J Ophthalmol.* 2010;94:611–615.
30. Chong NH, Keonin J, Luthert PJ, et al. Decreased thickness and integrity of the macular elastic layer of Bruch's membrane correspond to the distribution of lesions associated with age-related macular degeneration. *Am J Pathol.* 2005;166:241–251.
31. Chan WM, Lai TY, Liu DT, Lam DS. Intravitreal bevacizumab (avastin) for choroidal neovascularization secondary to central serous chorioretinopathy, secondary to punctate inner choroidopathy, or of idiopathic origin. *Am J Ophthalmol.* 2007; 143:977–983.
32. Lalwani GA, Rosenfeld PJ, Fung AE, et al. A variable-dosing regimen with intravitreal ranibizumab for neovascular age-related macular degeneration: year 2 of the PrONTO Study. *Am J Ophthalmol.* 2009;148:43–58, e41.
33. Chung SE, Kang SW, Lee JH, Kim YT. Choroidal thickness in polypoidal choroidal vasculopathy and exudative age-related macular degeneration. *Ophthalmology.* 2011;118:840–845.
34. Koizumi H, Yamagishi T, Yamazaki T, Kawasaki R, Kinoshita S. Subfoveal choroidal thickness in typical age-related macular degeneration and polypoidal choroidal vasculopathy. *Graefes Arch Clin Exp Ophthalmol.* 2011;249:1123–1128.
35. Jirarattanasopa P, Ooto S, Nakata I, et al. Choroidal thickness, vascular hyperpermeability, and complement factor H in age-related macular degeneration and polypoidal choroidal vasculopathy. *Invest Ophthalmol Vis Sci.* 2012;53:3663–3672.

SCIENTIFIC REPORTS

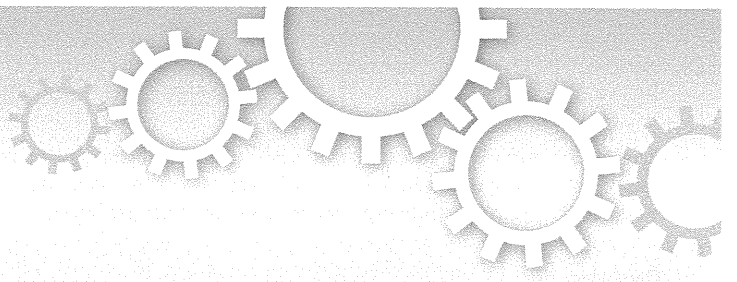

OPEN

SUBJECT AREAS:
MACULAR DEGENERATION
GENETIC PREDISPOSITION TO DISEASE

Received
11 November 2014

Accepted
27 February 2015

Published
20 March 2015

Correspondence and requests for materials should be addressed to K.Y. (yamashro@kuhp.kyoto-u.ac.jp)

Calcium, *ARMS2* Genotype, and *Chlamydia Pneumoniae* Infection in Early Age-Related Macular Degeneration: a Multivariate Analysis from the Nagahama Study

Isao Nakata[1,2], Kenji Yamashiro[1], Takahisa Kawaguchi[2], Hideo Nakanishi[1,2], Yumiko Akagi-Kurashige[1,2], Masahiro Miyake[1,2], Akitaka Tsujikawa[1], Ryo Yamada[2], Fumihiko Matsuda[2], Nagahisa Yoshimura[1] & Nagahama Study Group

[1]Department of Ophthalmology, Kyoto University Graduate School of Medicine, Kyoto, Japan, [2]Center for Genomic Medicine/Inserm U.852, Kyoto University Graduate School of Medicine, Kyoto, Japan.

Although various risk factors have been identified for the development of age-related macular degeneration (AMD), risk factors of early AMD have been relatively under studied. We aimed to investigate AMD risk factors by evaluating multiple factors in association with large drusen, an important component of AMD, simultaneously. In a community-based cross-sectional survey in Japan, 971 large drusen cases and 3,209 controls were compared for 65 variables, including systemic, environmental, and genetic factors. The association and the effect size of each factor were evaluated with logistic regression analysis using a backward-elimination approach. Multivariate analyses identified a significant association in serum calcium level (odds ratio [OR] = 0.932, $P = 1.05 \times 10^{-3}$), *ARMS2* A69S (rs10490924) genotype (OR = 1.046, $P < 0.001$), *Chlamydia pneumoniae* IgG (OR = 1.020, $P = 0.0440$), and age (OR= 1.013, $P < 0.001$) for large drusen. Hypocalcemia was observed in 7.2% of large drusen cases and in 5.5% of controls ($P = 0.0490$). *C. pneumoniae* infections was more frequent in large drusen cases (56.4%) than in conrols (51.7%, $P = 0.00956$). These results suggest that calcium, *ARMS2* genotype, *C. pneumonia* infection, and age are significant factors in the development of the early stages of AMD.

Age-related macular degeneration (AMD) is the leading cause of blindness among the elderly population in developed countries[1]. Early signs of AMD are characterized by drusen, small extracellular deposits between the retinal pigment epithelium (RPE) and the inner collagenous layer of Bruch's membrane, or by pigment abnormalities in the RPE in the macula[1]. Although visual symptoms are generally inconspicuous in the early stages of AMD[2], the presence of early signs is highly associated with the progression to advanced AMD, in which visual function is severely damaged[3]. Because the treatment options for advanced AMD is still limited and the associated economic burden is increasing[4], studying and preventing disease progression during the early stages of AMD are of increasing importance.

Age, smoking, and mutations in several genes are the most consistently identified risk factors for AMD[1]. These associations have been confirmed in populations across the globe, including Western and Asian countries[5–9]. To date, various other factors have been suggested to increase the risk of AMD[10–13]. However, the evidence and strength of these associations remain controversial[14–16]. The pathophysiology of AMD is still poorly understood and considered to be a constellation of diseases of varying etiologies.

Identifying the "true" risk factors for complex diseases such as AMD is a daunting task because multiple factors, including systemic, environmental, and genetic factors, contribute to disease liability with a small effect size. In fact, by analyzing a large number of subjects, recent genetic studies for complex diseases revealed several loci with smaller effect sizes, such as odds ratios (ORs) of 1.08–1.16[17]. To identify risk factors of complex disease and to determine the significance of each factor, a simultaneous analysis of multiple factors using a large number of subjects is necessary. In the present study, we sought to simultaneously investigate multiple risk factors for large

drusen, an important early sign of AMD that has been shown in many longitudinal studies to be predictive of incident AMD advanced[3,18], using a relatively large number of Japanese adults.

Results

Multivariate analysis for drusen. The distributions of predominant characteristics according to 971 large drusen cases and 3,209 controls are shown in Table 1. Study cases were significantly older than controls (65.1 ± 5.9 and 61.7 ± 6.5 years, respectively; $P < 0.001$). In the genetic analyses, a significant association was found between *ARMS2* A69S (rs10490924) and drusen; the frequency of the minor allele T, which is known as a risk allele for developing advanced AMD, was significantly higher in cases than in controls ($P < 0.001$). Conversely, *CFH* Y402H (rs1061170) and *CFH* I62V (rs800292) did not show a significant association with drusen ($P > 0.05$).

Each subject was tested for 65 factors, including 60 systemic factors, smoking status, Brinkman index, and the genetic factors *ARMS2* A69S, *CFH* Y402H, and *CFH* I62V (Table S1). After excluding two correlated variables (e.g., *C. pneumoniae* IgA and C-telopeptides crosslinks in lieu of the *C. pneumoniae* IgG and N-telopeptides crosslinks, respectively), 63 systemic factors were compared between cases and controls using univariate analyses. With this screening, a total of 29 factors, including age, systolic blood pressure, and genetic factors *ARMS2* A69S and *CFH* I62V, showed a potential association with drusen ($P < 0.25$; Table S2). Stepwise selection using a backward-elimination approach was performed for the 29 factors after adding five more previously reported AMD risk factors (BMI[11], HDL cholesterol[12], hs-CRP[13], smoking status, and *CFH* Y402H genotype). Table 2 summarizes the final multivariate analysis of all candidate predictor variables selected by stepwise analysis. Of the nine candidates, seven showed a significant association with drusen ($P < 0.05$): age, *ARMS2* A69S genotype, serum calcium, HDL cholesterol, α1-antitrypsin (AAT), hs-CRP, and *C. pneumoniae* IgG. Figure 1 shows the relative strength of each significant factor for drusen. We found that four of seven factors have a strong effect on the development of drusen: serum calcium level (OR 0.932, 95% confidential interval [CI] 0.894–0.972), *ARMS2* A69S (rs10490924) genotype (OR 1.046, 95%CI 1.025–1.069), *C. pneumoniae* IgG (OR 1.020, 95%CI 1.001–1.040), and age (OR 1.013, 95%CI 1.011–1.015).

Calcium level distribution and *C. pneumoniae* infection. Serum calcium levels in drusen cases were significantly lower than controls (9.05 and 9.11 mg/dL, respectively; $P < 0.001$). When applying the normal range of serum calcium (8.6–10.3 mg/dL), hypocalcemia (calcium level <8.6 mg/dL) was more frequent in the large drusen cases than in controls; 7.2% in drusen cases and 5.5% in controls, respectively ($P = 0.0490$; Table 3).

C. pneumoniae IgG levels were significantly elevated in drusen cases compared with controls (1.30 and 1.23, respectively; $P < 0.001$). We also confirmed a higher frequency of *C. pneumoniae* infections in drusen cases (56.4%) compared with controls (51.7%; $P = 0.00956$) by measuring serum reactivity according to the standard cutoff index for the IgG titer: <0.9, negative; 0.9 to 1.1, equivocal; and >1.1, positive (Table 3).

Discussion

With multivariate analysis considering 65 variables that include previously suggested AMD risk factors of systemic[10–13], genetic[7,19,20], and environmental factors, we found a strong effect of serum calcium level, *ARMS2* A69S genotype, age, and *C. pneumonia* infection on the development of drusen. While *ARMS2* genotype, age, *C. pneumonia* infection have previously been reported to be associated with AMD[1,21–23], no study has reported the association between serum calcium level and AMD. Serum calcium levels are under tight hormonal control with a normal range of 8.6–10.3 mg/dL. Calcium plays a key role in membrane potential, which is important for muscle contraction, heart rate regulation, and nerve impulse generation. Hypocalcemia is caused by loss of calcium from, for example, renal failure, or insufficient entry of calcium into the circulation, due to hypoparathyroidism, magnesium depletion, etc. In the present study, we found that hypocalcemia was more frequent in large drusen cases than in controls ($P = 0.0490$). The reason for the association between low calcium level and AMD is not clear; however, the presence of calcium in drusen has been known as early as 1987 by using classic freeze-fracture and scanning electron microscope based elemental analysis[24]. Moreover, a recent study showed that calcium is present in very high concentration in drusen[25]. It has also been reported that basal ganglia calcification often occurs in idiopathic hypoparathyroidism patients and is correlated with hypocalcemia, choroid plexus

Table 1 | Predominant Characteristics of the Study Subjects

	Large drusen	Control	*P*-value
N	971	3209	
Age, y	65.1 ± 5.9	61.7 ± 6.5	< 0.001
Sex, n (%)			
Male	357 (36.8)	1121 (34.9)	0.295
Female	614 (63.2)	2088 (65.1)	
Smoking, n (%)			
Never	646 (66.5)	2127 (66.3)	0.856
Past	201 (20.7)	687 (21.4)	
Current	124 (12.8)	395 (12.3)	
Brinkman index*	187.2 ± 360.7	173.2 ± 343.8	0.272
ARMS2 A69S, n (%)			
GG	239 (35.0)	1065 (43.5)	< 0.001
GT	334 (49.0)	1102 (45.0)	
TT	109 (16.0)	284 (11.6)	
CFH Y402H, n (%)			
CC	591 (87.2)	2122 (86.8)	0.908
CT	81 (11.9)	315 (12.9)	
TT	6 (0.9)	8 (0.3)	
CFH I62V, n (%)			
GG	241 (35.3)	927 (37.8)	0.147
GA	328 (48.1)	1163 (47.5)	
AA	113 (16.6)	361 (14.7)	

*The Brinkman index was calculated as daily number of cigarettes × years smoking.

Table 2 | Summary of the Multivariate Analyses for Large Drusen

	Beta	SE	OR (95%CI)	*P*-value
Age	0.013	0.001	1.013 (1.011–1.015)	< 0.001
ARMS2 A69S genotype	0.045	0.011	1.046 (1.025–1.069)	< 0.001
Calcium	−0.070	0.021	0.932 (0.894–0.972)	1.05×10^{-3}
HDL cholesterol	0.001	<0.001	1.001 (1.000–1.002)	2.07×10^{-3}
α1-Antitrypsin	0.001	<0.001	1.001 (1.000–1.002)	0.0268
Hs-CRP	<0.001	<0.001	1.000 (1.000–1.000)	0.0369
Chlamydia pneumoniae antibody, IgG	0.020	0.010	1.020 (1.001–1.040)	0.0440
CFH I62V genotype	0.017	0.010	1.017 (0.997–1.039)	0.100
Weed pollens allergy specific IgE	−0.016	0.010	0.984 (0.964–1.004)	0.113

SE, standard error; OR, odds ratio; HDL, high-density lipoprotein; Hs-CRP, high-sensitivity C-reactive protein; IgG, immunoglobulin G; IgE, immunoglobulin E.

calcification, and cataracts[26]. Although further studies are required, similar disease processes may affect calcification of the subretinal space, leading to the development of drusen, and a central nervous system with poor calcium control.

In the present study, we confirmed the association of age, *ARMS2* A69S genotype, HDL cholesterol, and hs-CRP levels with drusen, which were previously suggested as AMD risk factors[1,12,13,19]. However, multivariate analysis revealed that the effect size of hs-CRP and HDL cholesterol for drusen development was quite small (Fig. 1). These results are not surprising because several population-based cohort studies showed a lack of association between these factors and AMD[14–16]. Similarly, although α1-antitrypsin showed a potential association for drusen, the effect of this factor on disease development was limited (OR = 1.001).

C. pneumonia exposure has been suggested to be associated with AMD[21–23]. Kalayoglu et al reported that *C. pneumoniae* DNA was identified in surgically removed neovascular tissue from eyes with AMD[27], but other studies, including a population-based study examining 3,654 adults, failed to find any association between *C. pneumoniae* antibody titers and AMD, thereby generating controversy[28–31]. However, in the present study assessing 60+ factors in 4,000+ adults, we found a strong effect of *C. pneumoniae* infection on drusen. To date, there is a consensus that the *CFH* gene is associated with advanced AMD[7,20]. CFH is known as the main soluble inhibitor of the alternative pathway, which prevents progression of the cascade by binding and inactivating complement component C3b[32]. Several complement system factors, their activators, and complement regulatory proteins were identified as cardinal constituents of drusen[8,33] although the association between the *CFH* and early AMD remains controversial[34,35]. *C. pneumoniae* activates the alternative complement pathway or induces a chronic inflammatory state, which might contribute to the pathogenesis of AMD[21–23]. The present study, which showed a significant relationship between *C. pneumoniae* and the development of drusen, would indicate the significant role of the complement pathway in the inflammatory process with the disease development. On the other hand, we did not find strong associations between *CFH* genotypes and drusen. Taken together, our result would suggest that the activation of the alternative complement pathway by *C. pneumoniae* might be more important than that by *CFH* gene variation in the early stages of AMD in Asians.

Limitations of the present study include its cross-sectional design. In the present study, the role of previously suggested AMD risk factors, such as blood pressure[10], BMI[11], HDL cholesterol[12], and hs-CRP[13], were found to be limited. Also, we found no significant association between smoking and large drusen although Brinkman index of the large drusen group tended to be higher than that of controls (187.2 vs 173.2). These associations should be studied in a prospective study that evaluates multiple risk factors in AMD. Another lim-

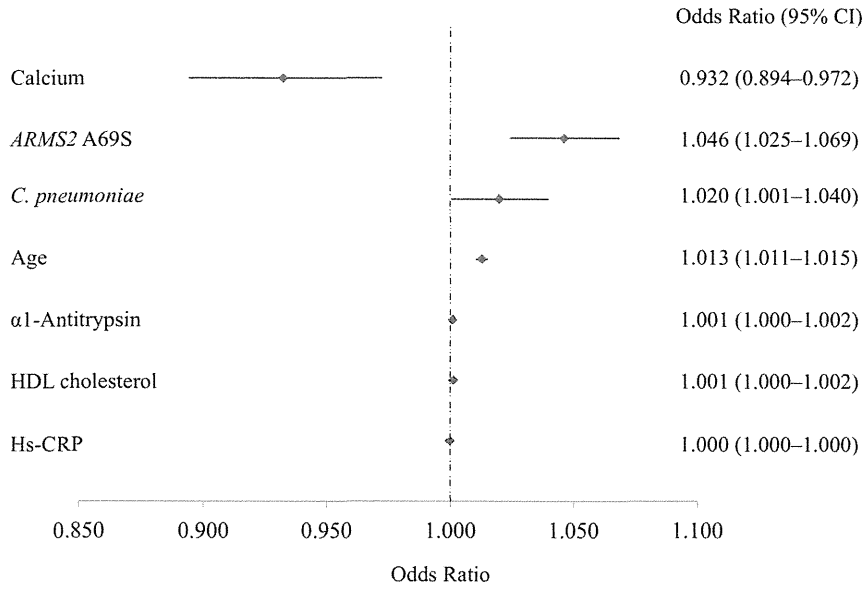

Figure 1 | The relative strength of the significant factors for large drusen that showed a significant association in the final multivariate analysis. Serum calcium level had the strongest effect on the development of large drusen; the other factors were *ARMS2* A69S (rs10490924) genotype, *Chlamydia pneumoniae* IgG, and age. High-density lipoprotein (HDL) cholesterol, α1-antitrypsin, and high-sensitivity C-reactive protein (hs-CRP) had limited effect on disease development with odds ratio between 1.000 and 1.001. A diamond represents the point estimate of odds ratio for each factor with a horizontal line of the 95% confidence interval (CI).

Table 3 | Status of the Serum Calcium Level and Chlamydia *Pneumoniae* infection in the Study Group

	Large drusen	Control	P-value
N	971	3209	
Serum calcium level (mg/dL)			
<8.6 (Hypocalcemia)	70 (7.2%)	177 (5.5%)	0.049
8.6–10.3 (Normal)	900 (92.8%)	3028 (94.4%)	0.0702
>10.3 (Hypercalcemia)	0 (0.0%)	4 (0.1%)	0.271
C. Pneumoniae IgG			
>1.1 (Positive infection)	548 (56.4%)	1659 (51.7%)	0.00956
0.9–1.1 (Equivocal)	109 (11.2%)	360 (11.2%)	0.995
<0.9 (Negative infection)	314 (32.4%)	1190 (37.1%)	0.00694

itation might be potential bias related to the high female to male ratio of the study subjects. However, a potential confounder in gender would be limited because a logistic regression analysis adjusting for gender was used in the present study. Further limitation is the lack of identifying a functional role of calcium in AMD. Although it is reported that calcium is present in very high concentration in drusen[25], there might be subretinal deposits without calcification that are currently called "drusen" by fundoscopy. Also, it remains unknown if low calcium intake can be the risk of the development of drusen. Following basic and clinical research investigating the role of calcium in AMD is therefore needed.

In summary, by simultaneous evaluation of multiple factors including systemic, environmental, and genetic factors, we found a strong association between serum calcium level, *ARMS2* A69S genotype, age, and *C. pneumonia* infection and the development of drusen. Our findings suggest a significant role for these factors during the early course of AMD.

Methods

The Nagahama Study Population. Participants were part of a study that was ancillary to the Nagahama Study, the details of which have been reported elsewhere[6]. The Nagahama Study is a community-based prospective cohort study designed to determine the prevalence and risk factors of various diseases in a community. Between November 2008 and November 2010, a total of 6,118 residents of Nagahama City aged ≥50 years participated in the Nagahama Study. All protocols and informed consent procedures were approved by the Kyoto University Graduate School and Faculty of Medicine Ethics Committee, the Ad Hoc Review Board of the Nagahama Cohort Project, and the Nagahama Municipal Review Board of Personal Information Protection. This study was carried out in accordance with the approved guidelines.

At baseline, all participants were asked to undergo eye examinations including automatic refractometry (Autorefractor ARK-530; Nidek Co Ltd, Aichi, Japan), axial length measurements (IOL Master; Carl Zeiss AG, Oberkochen, Germany), and fundus photography using a digital retinal camera (CR-DG10; Canon Inc., Tokyo, Japan) in a darkened room. All study subjects (n = 5,595) satisfied the following criteria: (a) age ≥50 years; (b) nonmydriatic fundus photographs for both eyes of sufficient quality for grading lesions; and (c) no other retinal diseases that would affect the precise grading of a macular lesion (such as diabetic retinopathy, retinal vein occlusion, or epiretinal membranes)[6]. Each fundus photograph was graded twice by two independent ophthalmologists for phenotypes of AMD through standardized grading procedures[3,6]. For the sake of multivariate analysis, we selected cases and controls from the study subjects. Based on the grading procedure, 971 individuals who had a large drusen (soft distinct and soft indistinct drusen ≥125 μm in diameter) in either eye were included as the study cases[36,37]. As controls, 3,209 individuals lacking any sign of AMD (drusen, retinal pigment epithelial abnormalities, or advanced AMD) in both eyes were selected. Twenty-nine cases with advanced AMD and a total of 1,386 individuals, including 276 with pigment epithelial abnormalities only and 1,110 with drusen less than 125 μm in diameter or reticular pseudodrusen, were excluded from the analysis.

Systemic Factor Analysis. A total of 60 systemic factors, including physical examination, hematological tests, biochemical tests, urinalysis, immunological tests, endocrinological tests, and allergy tests, were analyzed in each subject (Table S1). Blood and urine collection and processing were performed according to a standard protocol (XE-2100 hematology analyzer; Sysmex Co Ltd, Hyogo, Japan and LABOSPECT 008 Hitachi automatic analyzer; Hitachi Ltd, Tokyo, Japan). When the result exceeded the detection range, it was examined using a dilution test. The results of allergy tests were categorized as class 0 to 6 (class 0 = no allergy and class 6 = severe allergy) in a standard manner. To assess the environmental effect, information on smoking status was obtained via a self-report questionnaire. Total smoking amount was ascertained using the Brinkman index[38], calculated as the daily number of cigarettes × years of smoking.

Genotyping. To assess the role of genetic factors for disease, genomic DNA was prepared from the peripheral blood of 4,201 subjects. The most robust AMD-associated variants, A69S (rs10490924) on *ARMS2*[19] and Y402H (rs1061170) and I62V (rs800292) on *CFH*[7,20], were genotyped using TaqMan single nucleotide polymorphism assay with the PRISM 7700 system (Applied Biosystems, Inc., Foster City, CA, USA) and Human610-Quad BeadChips and HumanOmni2.5 BeadChips (Illumina, Inc., San Diego, CA, USA).

Statistical Analysis. Descriptive statistics are presented, and estimates of center and dispersion are described as mean and standard deviation (SD). To compare demographic characteristics, analysis of variance (ANOVA) or the χ^2 test were used.

For multivariate analysis, independent factors associated with drusen were determined using logistic regression. At first, univariate analyses were conducted to screen independent variables for a potential association with drusen. Since correlated variables should not be entered together in the same multivariable model, collinear variables were excluded from the analyses; for example, the variable for immunoglobulin A (IgA) antibodies for *Chlamydia pneumoniae* was excluded in lieu of the immunoglobulin G (IgG) antibodies for *C. pneumoniae*. Variables with $P < 0.25$ in the univariate analysis were entered in the multivariable analysis along with other predictors previously reported as being significantly associated with AMD (e.g., blood pressure[10], body mass index [BMI][11], high-density lipoprotein [HDL] cholesterol[12], high-sensitivity C-reactive protein [hs-CRP][13], smoking status, and the genetic factors). The final multivariate model was built through stepwise selection using a backward-elimination approach. Software R (http://www.r-project.org/) was used for statistical analyses. P values < 0.05 were considered statistically significant.

1. de Jong, P. T. Age-related macular degeneration. *N Engl J Med* **355**, 1474–85 (2006).
2. Hogg, R. E. & Chakravarthy, U. Visual function and dysfunction in early and late age-related maculopathy. *Prog Retin Eye Res* **25**, 249–76 (2006).
3. Ferris, F. L. *et al.* A simplified severity scale for age-related macular degeneration: AREDS Report No. 18. *Arch Ophthalmol* **123**, 1570–4 (2005).
4. Day, S., Acquah, K., Lee, P. P., Mruthyunjaya, P. & Sloan, F. A. Medicare costs for neovascular age-related macular degeneration, 1994-2007. *Am J Ophthalmol* **152**, 1014–20 (2011).
5. Smith, W., Mitchell, P. & Leeder, S. R. Smoking and age-related maculopathy. The Blue Mountains Eye Study. *Arch Ophthalmol* **114**, 1518–23 (1996).
6. Nakata, I. *et al.* Prevalence and characteristics of age-related macular degeneration in the Japanese population: the nagahama study. *Am J Ophthalmol* **156**, 1002–1009.e2 (2013).
7. Hageman, G. S. *et al.* A common haplotype in the complement regulatory gene factor H (HF1/CFH) predisposes individuals to age-related macular degeneration. *Proc Natl Acad Sci U S A* **102**, 7227–32 (2005).
8. Gold, B. *et al.* Variation in factor B (BF) and complement component 2 (C2) genes is associated with age-related macular degeneration. *Nat Genet* **38**, 458–62 (2006).
9. Nakata, I. *et al.* Significance of C2/CFB Variants in Age-Related Macular Degeneration and Polypoidal Choroidal Vasculopathy in a Japanese Population. *Invest Ophthalmol Vis Sci* **53**, 794–8 (2012).
10. Hyman, L., Schachat, A. P., He, Q. & Leske, M. C. Hypertension, cardiovascular disease, and age-related macular degeneration. Age-Related Macular Degeneration Risk Factors Study Group. *Arch Ophthalmol* **118**, 351–8 (2000).
11. Seddon, J. M., Cote, J., Davis, N. & Rosner, B. Progression of age-related macular degeneration: association with body mass index, waist circumference, and waist-hip ratio. *Arch Ophthalmol* **121**, 785–92 (2003).
12. Tan, J. S., Mitchell, P., Smith, W. & Wang, J. J. Cardiovascular risk factors and the long-term incidence of age-related macular degeneration: the Blue Mountains Eye Study. *Ophthalmology* **114**, 1143–50 (2007).

13. Boekhoorn, S. S., Vingerling, J. R., Witteman, J. C., Hofman, A. & de Jong, P. T. C-reactive protein level and risk of aging macula disorder: The Rotterdam Study. *Arch Ophthalmol* **125**, 1396–401 (2007).
14. Klein, R. *et al.* Early age-related maculopathy in the cardiovascular health study. *Ophthalmology* **110**, 25–33 (2003).
15. Tomany, S. C. *et al.* Risk factors for incident age-related macular degeneration: pooled findings from 3 continents. *Ophthalmology* **111**, 1280–7 (2004).
16. Buch, H. *et al.* Risk factors for age-related maculopathy in a 14-year follow-up study: the Copenhagen City Eye Study. *Acta Ophthalmol Scand* **83**, 409–18 (2005).
17. Park, J. H. *et al.* Distribution of allele frequencies and effect sizes and their interrelationships for common genetic susceptibility variants. *Proc Natl Acad Sci U S A* **108**, 18026–31 (2011).
18. Klein, R., Klein, B. E., Jensen, S. C. & Meuer, S. M. The five-year incidence and progression of age-related maculopathy: the Beaver Dam Eye Study. *Ophthalmology* **104**, 7–21 (1997).
19. Jakobsdottir, J. *et al.* Susceptibility genes for age-related maculopathy on chromosome 10q26. *Am J Hum Genet* **77**, 389–407 (2005).
20. Hayashi, H. *et al.* CFH and ARMS2 variations in age-related macular degeneration, polypoidal choroidal vasculopathy, and retinal angiomatous proliferation. *Invest Ophthalmol Vis Sci* **51**, 5914–9 (2010).
21. Kalayoglu, M. V., Galvan, C., Mahdi, O. S., Byrne, G. I. & Mansour, S. Serological association between Chlamydia pneumoniae infection and age-related macular degeneration. *Arch Ophthalmol* **121**, 478–82 (2003).
22. Ishida, O. *et al.* Is Chlamydia pneumoniae infection a risk factor for age related macular degeneration? *Br J Ophthalmol* **87**, 523–4 (2003).
23. Robman, L. *et al.* Exposure to Chlamydia pneumoniae infection and progression of age-related macular degeneration. *Am J Epidemiol* **161**, 1013–9 (2005).
24. Ulshafer, R. J., Allen, C. B., Nicolaissen, B. & Rubin, M. L. Scanning electron microscopy of human drusen. *Invest Ophthalmol Vis Sci* **28**, 683–9 (1987).
25. Flinn, J. M., Kakalec, P., Tappero, R., Jones, B. & Lengyel, I. Correlations in distribution and concentration of calcium, copper and iron with zinc in isolated extracellular deposits associated with age-related macular degeneration. *Metallomics* **6**, 1223–8. (2014).
26. Goswami, R. *et al.* Prevalence and progression of basal ganglia calcification and its pathogenic mechanism in patients with idiopathic hypoparathyroidism. *Clin Endocrinol (Oxf)* **77**, 200–6 (2012).
27. Kalayoglu, M. V. *et al.* Identification of Chlamydia pneumoniae within human choroidal neovascular membranes secondary to age-related macular degeneration. *Graefes Arch Clin Exp Ophthalmol* **243**, 1080–90 (2005).
28. Robman, L. *et al.* Exposure to Chlamydia pneumoniae infection and age-related macular degeneration: the Blue Mountains Eye Study. *Invest Ophthalmol Vis Sci* **48**, 4007–11 (2007).
29. Miller, D. M. *et al.* The association of prior cytomegalovirus infection with neovascular age-related macular degeneration. *Am J Ophthalmol* **138**, 323–8 (2004).
30. Haas, P. *et al.* Complement factor H gene polymorphisms and Chlamydia pneumoniae infection in age-related macular degeneration. *Eye (Lond)* **23**, 2228–32 (2009).
31. Klein, R. *et al.* Systemic markers of inflammation, endothelial dysfunction, and age-related maculopathy. *Am J Ophthalmol* **140**, 35–44 (2005).
32. Despriet, D. D. *et al.* Complement factor H polymorphism, complement activators, and risk of age-related macular degeneration. *JAMA* **296**, 301–9 (2006).
33. Anderson, D. H., Mullins, R. F., Hageman, G. S. & Johnson, L. V. A role for local inflammation in the formation of drusen in the aging eye. *Am J Ophthalmol* **134**, 411–31 (2002).
34. Chen, J. H. *et al.* No association of age-related maculopathy susceptibility protein 2/HtrA serine peptidase 1 or complement factor H polymorphisms with early age-related maculopathy in a Chinese cohort. *Mol Vis* **19**, 944–54 (2013).
35. Holliday, E. G. *et al.* Insights into the genetic architecture of early stage age-related macular degeneration: a genome-wide association study meta-analysis. *PLoS One* **8**, e53830 (2013).
36. Oshima, Y. *et al.* Prevalence of age related maculopathy in a representative Japanese population: the Hisayama study. *Br J Ophthalmol* **85**, 1153–7 (2001).
37. Yasuda, M. *et al.* Nine-year incidence and risk factors for age-related macular degeneration in a defined Japanese population the Hisayama study. *Ophthalmology* **116**, 2135–40 (2009).
38. Brinkman, G. L. & Coates, E. O. The effect of bronchitis, smoking, and occupation on ventilation. *Am Rev Respir Dis* **87**, 684–93 (1963).

Acknowledgments

We thank the participants of the Nagahama Study, Nagahama City Office, and the nonprofit organization Zero-ji Club for Health Promotion. The following investigators are core members of the Nagahama Study Group: Takeo Nakayama (Department of Health Informatics, Kyoto University School of Public Health, Kyoto, Japan), Akihiro Sekine (Department of Genome Informatics, Kyoto University School of Public Health, Kyoto, Japan), Shinji Kosugi (Department of Medical Ethics, Kyoto University School of Public Health, Kyoto, Japan), Yasuharu Tabara (Center for Genomic Medicine, Graduate School of Medicine, Kyoto University), and Michiaki Mishima (Department of Respiratory Medicine, Kyoto University Graduate School of Medicine, Kyoto, Japan). This study was partly supported by grants-in-aid from the following organizations: the Ministry of Education, Culture, Sports, Science and Technology of Japan (2006–2012); the Japan Society for the Promotion of Science (Nos. 19390442, 22791706, and 22791653); the Japanese National Society for the Prevention of Blindness; and the Takeda Science Foundation (2008–2012). The funders had no role in study design, data collection and analysis, decision to publish, or preparation of the manuscript.

Author contributions

I.N., K.Y., F.M. and N.Y. have designed the study. I.N., K.Y., H.N., Y.A-K., M.M., F.M. and NSG acquired the data. I.N., T.K. and R.Y. analyzed and interpreted data. K.Y., A.T. and N.Y. supervised the study. I.N. wrote the manuscript. All authors reviewed the manuscript.

Additional information

The list of authors in the Nagahama Study Group: T.N., A.S., S.K., Y.T., and M.M.

Supplementary information accompanies this paper at http://www.nature.com/scientificreports

Competing financial interests: The authors declare no competing financial interests.

How to cite this article: Nakata, I. *et al.* Calcium, *ARMS2* Genotype, and *Chlamydia Pneumoniae* Infection in Early Age-Related Macular Degeneration: a Multivariate Analysis from the Nagahama Study. *Sci. Rep.* 5, 9345; DOI:10.1038/srep09345 (2015).

Choroidal Neovascularization in Eyes With Choroidal Vascular Hyperpermeability

Masahiro Miyake,[1,2] Akitaka Tsujikawa,[1] Kenji Yamashiro,[1] Sotaro Ooto,[1] Akio Oishi,[1] Hiroshi Tamura,[1] Isao Nakata,[1,2] Fumihiko Matsuda,[2] and Nagahisa Yoshimura[1]

[1]Department of Ophthalmology and Visual Sciences, Kyoto University Graduate School of Medicine, Kyoto, Japan
[2]Center for Genomic Medicine/Inserm U.852, Kyoto University Graduate School of Medicine, Kyoto, Japan

Correspondence: Akitaka Tsujikawa, Department of Ophthalmology and Visual Sciences, Kyoto University Graduate School of Medicine, Sakyo-ku, Kyoto 606-8507, Japan; tujikawa@kuhp.kyoto-u.ac.jp.

Submitted: January 29, 2014
Accepted: April 17, 2014

Citation: Miyake M, Tsujikawa A, Yamashiro K, et al. Choroidal neovascularization in eyes with choroidal vascular hyperpermeability. *Invest Ophthalmol Vis Sci.* 2014;55:3223-3230. DOI:10.1167/iovs.14-14059

Purpose. We describe the clinical and genetic characteristics of choroidal neovascularization (CNV) in eyes with choroidal vascular hyperpermeability (CVH).

Methods. This cross-sectional study consisted of 438 consecutive patients who underwent fluorescein and indocyanine green angiography for macular disease. We used the genotypes of 1576 age-related macular degeneration (AMD) cases and 3248 general population controls as reference groups for genetic association analyses.

Results. Of 871 eyes (438 patients) examined, CVH was found in 227 eyes (26.1%). Of these 227 eyes, 52 (22.6%) had CNV in the macular area. The proportion of patients with drusen and the choroidal thickness were not different between eyes with and without CNV, after adjusting for age ($P = 0.21$ and 0.95). Of the 52 eyes with CNV, 51 had type 1 CNV and only one eye had pure type 2 CNV. Of the 51 eyes with type 1 CNV, polypoidal lesions were observed in 17 eyes (33.3%). Genotype distributions of *ARMS2* (A69S) and *CFH* (I62V) in patients with CVH and type 1 CNV significantly differed from those of AMD cases ($P = 0.0014$ and 0.0098, respectively), but not from general population controls ($P = 0.33$ and 0.82, statistical power of 88.5% and 72.9%, respectively).

Conclusions. In patients with CVH, type 1 CNV may occur frequently and sometimes accompanies type 2 CNV or polypoidal lesions. In terms of *ARMS2* and CFH, genetic background of patients with CVH and type 1 CNV was different from those with AMD, but rather similar to the general Japanese population.

Keywords: CSC, type 1 CNV, choroidal vascular hyperpermeability, AMD, genetics

Central serous chorioretinopathy (CSC) is characterized by a serous retinal detachment in the macular area, as confirmed by leakage on fluorescein angiogram (FA). In most eyes with CSC, indocyanine green angiography (ICGA) shows choroidal vascular abnormalities, including choroidal filling delays, dilated vasculature, punctate hyperfluorescent spots, and/or choroidal vascular hyperpermeability (CVH).[1-6] It has been reported that CVH occurs in 90% to 100% of eyes with CSC,[5,7-11] persisting even after serous retinal detachment resolution.[8,11] Interestingly, disease recurrence with new leakage often is seen in the area of CVH.[8,11] In addition, it generally is believed that CVH underlies pathophysiologic abnormalities associated with CSC.

It was noted recently that CVH sometimes is observed in eyes with neovascular age-related macular degeneration (AMD)[12] and polypoidal choroidal vasculopathy (PCV).[12-14] Several studies also have associated CVH with phenotypic variability and AMD treatment efficacy. Jirarattanasopa et al.[12] reported that eyes with AMD or PCV that also had CVH had a thicker choroid. Koizumi et al.[14] reported that anti-VEGF treatments were less effective in eyes with PCV accompanied by CVH. However, Maruko et al.[15] found that photodynamic therapy was more effective in eyes with PCV and CVH. These features are consistent with typical CSC characteristics.[2,4,10,16]

It is thought classically that CSC is not accompanied by choroidal neovascularization (CNV) and that patients have a good visual prognosis. In a retrospective study by Mudvari et al.,[17] none of the 340 consecutive CSC patients developed CNV during an approximately 4-year follow-up period (mean of 49 months). However, Spaide et al.[4] reported that older patients with CSC had a lower visual acuity (VA), and were more likely to have diffuse retinal pigment epitheliopathy and secondary CNV than their younger counterparts. Subsequent reports have suggested that classic CNV (mainly type 2) and polypoidal lesions are possible complications of CSC and may contribute to visual loss in these eyes.[5,18-21] Fung et al.[22] recently described 9 eyes with longstanding CSC that went on to develop type 1 CNV. They concluded that a portion of these eyes were given a diagnosis of neovascular AMD, but should have been given a diagnosis of CNV secondary to CSC (i.e., CNV masquerading as AMD).

It still is controversial whether CNV that shares features with CSC originally is AMD or CSC. However, based on the above reports, we hypothesized that most of "AMD with CVH" might truly be "CNV secondary to CSC" masquerading as AMD. Here, to recruit "AMD with CVH" and "CNV secondary to CSC" as one cluster of CNV, we studied consecutive eyes with "CNV with CVH." Although most of these CNV are diagnosed currently as AMD, we demonstrated this cluster of CNV has different characteristics from AMD.

Methods

The current study was approved by the Institutional Review Board (IRB) at Kyoto University Graduate School of Medicine and all study conduct adhered to the tenets of the Declaration of Helsinki. Written informed consent was obtained from each patient who was genotyped. According to our IRB guidelines, it was not mandatory to obtain informed consent from patients before retrospectively reviewing their medical records.

Subjects

We retrospectively reviewed the medical records of 438 consecutive patients who visited the macular service at Kyoto University Hospital (Kyoto, Japan) between June 2011 and December 2012, and who underwent FA and ICGA to confirm or rule out macular diseases (e.g., AMD, CSC, other CNV, or other diseases requiring angiography for diagnosis). Comprehensive ophthalmic examinations were conducted on all patients, which included best-corrected VA, dilated indirect and contact lens slit-lamp biomicroscopy, automatic objective refraction, color fundus photography, FA, and ICGA using a confocal laser scanning ophthalmoscope (HRA2; Heidelberg Engineering, Dossenheim, Germany). Spectral-domain optical coherence tomography (SD-OCT, Spectralis; Heidelberg Engineering) also was performed on all patients. All images were obtained using an eye-tracking system, and 100 scans were averaged automatically to improve the signal-to-noise ratio. Inverted images were obtained routinely in all patients using an enhanced-depth imaging (EDI) technique introduced by Spaide et al.[23]

CVH and Other Findings

The CVH was evaluated in the late phase of ICGA, approximately 10 to 15 minutes after dye injection. With reference to a report by Guyer et al.,[1] CVH was defined as multifocal areas of hyperfluorescence with blurred margins within the choroid, followed by minimal extension of focal hyperfluorescent area (Fig. 1). This status was evaluated by two retina specialists (MM, AT) who were masked to all other medical information. Both evaluators diagnosed CVH as a binary trait (i.e., present or not), and only the eyes that both evaluators diagnosed with CVH were considered CVH-positive in further analyses. After recruitment, complications were evaluated in all eyes with CVH. Complications, such as type 1 CNV, type 2 CNV, and polypoidal lesion, were determined based on the results of fundus examination, FA, ICGA, and OCT by two retina specialists (MM and AT).

For patients who were judged to have CVH in at least one eye, we evaluated EDI-OCT images in both eyes. Central subfoveal choroidal thickness, defined as the vertical distance between Bruch's membrane and the choriosclera interface, was measured manually by a retinal specialist blinded to study parameters using the built-in caliber. We used data from horizontal line scans. If it was difficult to identify the outer choroid in its entirety, we chose 10 points at which the choriosclera interface could be identified easily and created a segmentation line, based on which subfoveal choroidal thickness was measured.

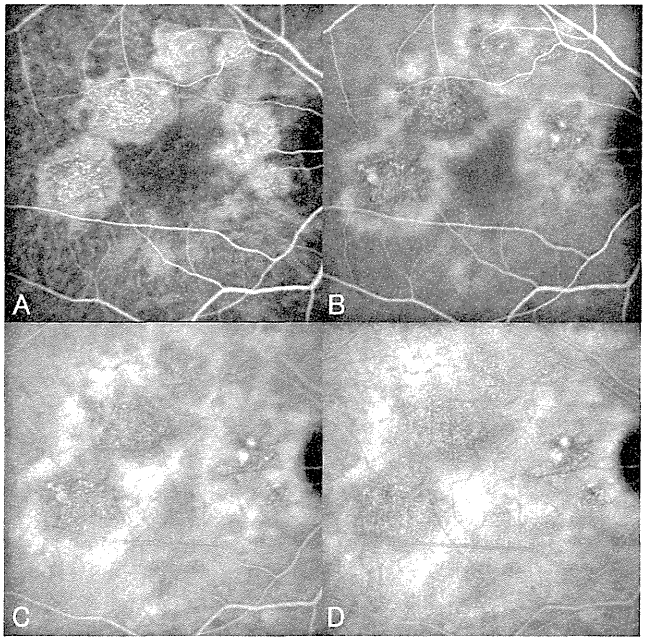

Figure 1. Typical CVH observed in a 43-year-old man. Four images from an ICGA obtained at 1:35:50 (**A**), 5:37:51 (**B**), 10:43:80 (**C**), and 16:17:16 (**D**) after the intravenous injection of indocyanine green. (**A**) In the early phase, clusters of small hyperfluorescent spots can be seen in focal areas of hyperfluorescence. (**B–D**) Focal areas of hyperfluorescence expand over time, eventually forming a ring shape. The center of the initially hyperfluorescent area gradually becomes hypofluorescent.

Genotyping

Genomic DNAs were prepared from peripheral blood using a DNA extraction kit (QuickGene-610L; Fujifilm, Minato, Tokyo, Japan). We selected two major AMD-associated single nucleotide polymorphisms (SNP), *compliment factor H (CFH)* I62V (rs800292),[24–26] and *age-related maculopathy susceptibility 2 (ARMS2)* A69S (rs10490924).[26–28] Samples from patients with CVH and CNV in at least one eye were genotyped using a commercially available assay (Taqman SNP assay with the ABI PRISM 7700 system; Applied Biosystems, Foster City, CA, USA).

For the reference group, we used two cohorts. One was the Kyoto AMD cohort, which consisted of 1576 unrelated AMD patients recruited from the Departments of Ophthalmology at Kyoto University Hospital, Fukushima Medical University

Table 1. Patient and Ocular Characteristics of Subjects With CVH

	No CNV	Any CNV	*P* Value	*P* Value Adjusted for Age
n	175	52	-	-
Age, y	59.6 ± 13.0	68.0 ± 11.2	<0.001	-
Sex, male:female	140:35	44:8	0.55	-
Serous PED (%)	49 (28.0)	7 (13.5)	0.037	0.21
Drusen (%)	43 (24.5)	21 (40.4)	0.028	0.25
Visual acuity, logMAR	−0.03 ± 0.21	0.28 ± 0.34	<0.001	<0.001
Choroidal thickness, μm	362.9 ± 120.1	323.6 ± 102.2	0.035	0.76

All data are presented as mean ± SD, where applicable. PED, pigment epithelial detachment, logMAR, logarithm of minimum angle resolution.

Investigative Ophthalmology & Visual Science

Table 2. Patient and Ocular Characteristics of Subjects With CVH and CNV

	Type 1 CNV						
	Pure Type 1 CNV	*P* Value* (Adjusted for Age)	With Type 2 CNV	*P* Value* (Adjusted for Age)	With Polypoidal Lesion	*P* Value* (Adjusted for Age)	Pure Type 2 CNV
n	28	-	6	-	17	-	1
Age, y	68.4 ± 9.2	<0.001	63.3 ± 15.5	0.34	70.1 ± 9.9	<0.001	33
Sex, male:female,	26:2	0.12	3:3	0.11	15:2	0.53	0:1
serous PED	4 (14.3%)	0.13 (0.48)	1 (16.7%)	0.55 (0.75)	2 (11.8%)	0.17 (0.57)	0
Drusen	11 (39.3%)	0.11 (0.36)	1 (16.7%)	066 (0.54)	9 (52.9%)	0.016 (0.072)	0
Visual acuity, logMAR	0.22 ± 0.26	<0.001 (<0.001)	0.45 ± 0.31	<0.001 (<0.001)	0.31 ± 0.46	<0.001 (<0.001)	0.22
Choroidal thickness, μm	353.3 ± 110.7	0.69 (0.15)	331.7 ± 62.5	0.53 (0.98)	268.5 ± 81.1	0.0039 (0.077)	327.0

Data presented as mean ± SD.
* Compared to eyes without CNV.

Hospital, and Kobe City Medical Center General Hospital. The AMD diagnosis was confirmed by 3 retinal specialists. A fourth specialist (NY) was consulted when the initial three reviewers could not reach a consensus. These patients were genotyped using Illumina OmniExpress or HumanOmni2.5M Arrays (Illumina, Inc., San Diego, CA, USA). Another cohort of the general population made up the control group and consisted of 3248 unrelated individuals, recruited from the Nagahama Prospective Genome Cohort for the Comprehensive Human Bioscience (The Nagahama Study).[29–31] These patients were genotyped using HumanHap610K Quad Arrays, HumanOmni2.5M Arrays, and/or HumanExome Arrays (Illumina, Inc.), and the two SNPs genotypes were extracted from the cohort's fixed dataset.

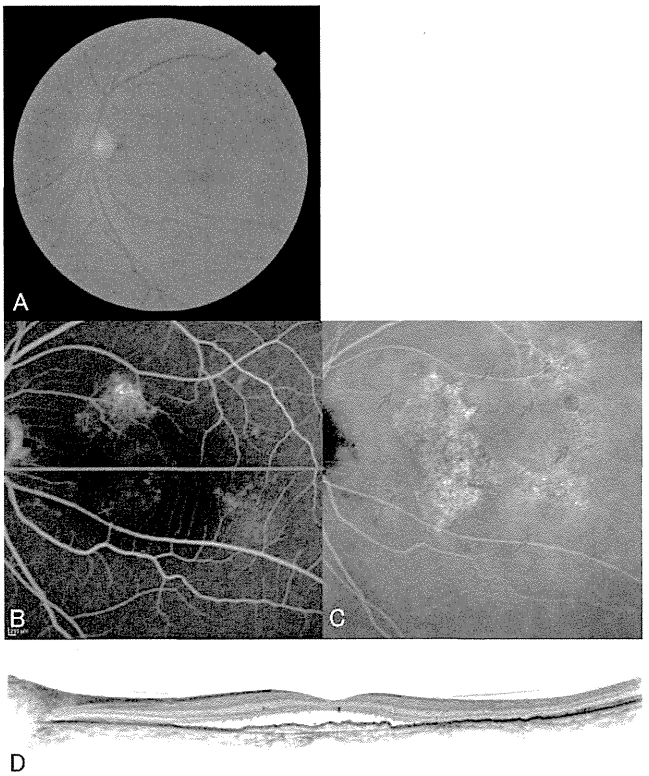

Figure 2. CVH with pure type 1 CNV. (**A**) A 70-year-old male with a serous retinal detachment in the left eye (VA = 20/40). (**B**) An FA showing occult CNV. (**C**) Late-phase ICGA showing typical CVH (*arrows*). (**D**) A horizontal OCT cross-sectional image reveals a subfoveal fibrovascular pigment epithelium detachment (type 1 CNV) with subretinal fluid. Neither a polypoidal lesion nor classic CNV is apparent in the angiogram.

Statistical Analysis

Every 2 × 2 table was compared using a Fisher's exact test, while continuous variables were compared using unpaired *t*-tests. Linear or logistic regression analyses were performed and adjusted for age. Genotypes were compared using χ^2 tests for trend. Statistical power of the genetic association test also was calculated. These statistical analyses were conducted using Software R (R Foundation for Statistical Computing, Vienna, Austria). A *P* value <0.05 was considered statistically significant.

Results

Of the 871 eyes (438 patients) examined, 120 eyes (61 patients) had high myopia (axial length ≥ 26 mm). No eyes with high myopia had signs of CVH on ICGA. In the current study, CVH was seen in 227 eyes (26.1%) from 141 patients (112 men, 29 women), ranging in age from 33 to 89 years (62.0 ± 13.1 years). All patients were Japanese and of Asian ancestry. Further analysis was performed on data from these 227 eyes with CVH.

Of the 227 eyes with CVH, 52 (22.6%) had CNV in the macular area. Table 1 summarizes the demographics of these eyes. The mean age of patients with CNV was significantly higher than that of subjects without CNV. The proportion of eyes with a serous pigment epithelium detachment (PED) or any drusen was higher in eyes with CNV. Measurements of choroidal thickness also seemed to be larger in eyes with CNV, but none of these differences was statistically significant after adjusting for age (PED $P = 0.34$, drusen $P = 0.21$, and choroidal thickness $P = 0.95$, respectively).

Table 2 shows subclassification of the 52 eyes with CVH and CNV. Of all eyes, 51 (22.6%) had type 1 CNV in the macular area (Fig. 2). Pure type 2 CNV, without any type 1 CNV, was seen in only one eye (0.4%) and data from this eye were excluded from all further analyses. Of the 51 eyes with type 1 CNV, polypoidal lesions were observed in 17 eyes (33.3%, Fig. 3), and type 2 CNV was observed in 6 eyes (11.8%, Fig. 4). The remaining 28 eyes (54.9%) had only type 1 CNV. The mean age of patients with either type 1 CNV or with polypoidal lesions was significantly higher than that of patients with no CNV, and their VA was significantly lower than that of eyes with no CNV. Additionally, more eyes with polypoidal lesions had concomitant drusen and thinner choroids than eyes without these